Mathematisches Forschungsinstitut Oberwolfach

Report No. 50/2016

DOI: 10.4171/OWR/2016/50

Mini-Workshop: Fast Solvers for Highly Oscillatory Problems

Organised by
Timo Betcke, London
Steffen Börm, Kiel
Sabine Le Borne, Hamburg
Per-Gunnar Martinsson, Boulder

30 October – 5 November 2016

Abstract. The efficient numerical solution of highly oscillatory problems is one of the grand challenges of Applied Mathematics with diverse applications across the natural sciences and engineering. This workshop brings together experts in domain based methods and integral equation methods to share novel ideas and to discuss challenges on the way to developing efficient solvers at high frequencies.

Mathematics Subject Classification (2010): 65xx.

Introduction by the Organisers

The fast solution of highly oscillatory problems remains one of the great challenges of applied and computational mathematics. This workshop brought together experts working on fast direct solvers for integral equations, preconditioning and domain decomposition methods to share novel ideas for the development of scalable frequency domain solvers for acoustic and electromagnetic problems.

The workshop was roughly divided into three broad subject areas, namely 1.) fast direct solvers for Helmholtz problems, 2.) fast iterative methods and preconditioning for oscillatory integral equations, and 3.) domain decomposition methods for volume problems.

The first day started off with an overview talk by Per-Gunnar Martinsson, outlining the challenges of developing fast direct solvers for high-frequency problems. We then had talks by Steffen Börm and Markus Melenk on novel directional $\mathcal{H}^2$ matrix techniques for highly oscillatory problems.

In the evening Timo Betcke led a discussion on large-scale industrial challenges for high-frequency solvers and the need to develop large-scale coupled FEM/BEM domain decomposition frameworks to address them.

The second day saw talks by Adrianna Gillman and Alex Barnett on fast direct solvers for oscillatory problems, and on the fast solution of periodic problems, respectively. The algorithms presented in these talks produced stunning results and were backed up by beautiful graphical visualizations of solutions of oscillatory problems in two and three space dimensions (see also the respective extended abstracts).

Significant discussions were created by Mike O'Neil's talk. He presented novel results on butterfly algorithms, and it was decided to devote the whole Wednesday afternoon to a more detailed understanding of butterfly algorithms. Butterfly compression has the potential to significantly improve the efficiency of fast direct solvers for oscillatory problems and a lot of work is currently going into the development of novel algorithms based on butterfly ideas.

A remarkable result of the butterfly discussions during the week was that directional $\mathcal{H}^2$ structures applied to individual admissible blocks lead to a butterfly representation. This opens up the potential to apply algorithmic developments for $\mathcal{H}^2$ matrices to butterfly decompositions.

Due to weather changes the traditional tour was done together with the other workshop groups already on Tuesday afternoon.

On Wednesday the focus shifted to fast multipole methods and preconditioning. Stéphanie Chaillat started with an overview talk on Fast Multipole Methods and various applications in elastodynamics, followed by a talk by Marion Darbas on novel analytic preconditioners for high-frequency elastic problems.

The talks were concluded on Wednesday by an overview presentation by Timo Betcke on the BEM++ software framework which provides solvers for a wide range of electrostatic, acoustic and electromagnetic problems. In the afternoon the aforementioned discussions on butterfly algorithms, led by Mike O'Neil took place.

Thursday started with the second part of Stéphanie Chaillat's overview talk on fast solvers for elastodynamics. This was followed by an overview by Sabine Le Borne on the use of fast hierarchical matrix solver techniques for integral equations in scattered data approximation problems.

The final talk of the day was an overview talk by Martin Gander on variants of optimized Schwarz domain decomposition solvers for high-frequency problems. His framework generalizes a range of methods, including sweeping preconditioners, polarized traces, and multitrace formulations. This sparked many discussions in the afternoon, leading over to Friday which concluded with talks by Ivan Graham on shifted Laplacian preconditioners and an introduction to the ideas behind polarized traces by Laurent Demanet, which provided a fitting conclusion to the workshop.

The workshop created a unique atmosphere to bring together fast solver experts from the domain decomposition and the boundary integral equation community.

The main threads that developed throughout the workshop were the efficient use of directional approximations and butterfly ideas, numerical and analytic DtN approximations for preconditioning and as transmission conditions in domain decomposition methods, and unifying domain decomposition frameworks that can incorporate a range of currently investigated methods. The format of the workshop allowed to exchange these ideas and give strong impulses for future research into fast high-frequency solvers.

Acknowledgement: The MFO and the workshop organizers would like to thank the National Science Foundation for supporting the participation of junior researchers in the workshop by the grant DMS-1049268, "US Junior Oberwolfach Fellows".

Mini-Workshop: Fast Solvers for Highly Oscillatory Problems

Table of Contents

Per-Gunnar Martinsson
High-order discretizations and direct solvers 2875

Steffen Börm (joint with Christina Börst)
$\mathcal{DH}^2$-matrix compression of Helmholtz problems 2879

Jens M. Melenk (joint with S. Börm)
Stability of iterated re-interpolation in high-frequency applications 2881

Adrianna Gillman (joint with P.G. Martinsson, A. Barnett, C. Borges and L. Greengard)
The Hierarchical Poincaré-Steklov scheme: Oscillatory problems 2884

Alex Barnett (joint with Min Hyung Cho, Yuxiang Liu, Adrianna Gillman, Jun Lai, Motoki Kobayashi, Leslie Greengard)
Robust periodization of frequency-domain integral equation solvers 2887

Michael O'Neil
Butterfly algorithms 2891

Stéphanie Chaillat
Fast solvers for 3D elastodynamic Boundary Element Methods 2892

Marion Darbas (joint with S. Chaillat, F. Le Louër)
Analytic preconditioners for 3D high-frequency elastic scattering problems 2894

Timo Betcke (joint with Matthew Scroggs, Wojciech Śmigaj)
Software operator frameworks for computational boundary element methods 2896

Sabine Le Borne
Hierarchical matrices in scattered data approximation 2898

Martin J. Gander
On the limitations of sweeping type preconditioners for wave propagation 2899

Ivan Graham (joint with Euan Space, Eero Vainikko)
On domain decomposition preconditioners for finite element approximations of the Helmholtz equation using absorption 2903

Laurent Demanet
Aide-mémoire: The method of polarized traces 2904

Abstracts

High-order discretizations and direct solvers

Per-Gunnar Martinsson

Context: The development of numerical methods for solving linear elliptic PDEs has in many ways reached a high degree of maturity. A broad range of versatile tools for discretizing the PDE, and solving the resulting linear systems have been developed. One area that remains challenging concerns certain problems with highly oscillatory solutions. As a simple model problem, consider an interior Helmholtz boundary value problem of the form

$$\begin{cases} -\Delta u(x) - \kappa^2 u(x) = f(x), & x \in \Omega, \\ u(x) = g(x), & x \in \Gamma, \end{cases} \tag{1}$$

where Ω is a domain in two or three dimensions with boundary Γ. The scalar κ is the *wavenumber*. The solution to (1) is typically oscillatory, with a wavelength of $2\pi/\kappa$. Despite its apparent simplicity, it remains a challenge to solve the equation (1) numerically when κ grows large. In part, this is to be expected since (1) can in this environment become ill-posed. For instance, for any value of κ such that κ^2 is an eigenvalue of $-\Delta$ on the domain Ω (with homogeneous Dirichlet boundary data), there are functions g for which (1) does not have a solution, and the solution is not unique. Moreover, when κ is *close* to an eigenvalue, the problem is numerically ill-conditioned in the sense that small changes to either the geometry or the boundary condition can result in large changes in the solution. Finally, the linear system of equations resulting upon discretization of (1) is challenging to solve using standard iterative solvers, since generic pre-conditioners have so far proven to be elusive.

Direct solvers: In the talk, we make a case that so called *direct solvers* provide a particularly promising tool for successfully solving problems with oscillatory solutions. In this context, we use the term "direct solver" to indicate a method that given some tolerance ε computes an approximation to the solution operator of (1) that given input data f and g computes the corresponding solution u to within tolerance ε. In other words, a direct solver builds a discrete approximation to the continuum solution operator

$$u(x) = \int_\Omega F(x,y)\, f(y)\, dy + \int_\Gamma G(x,y)\, g(y)\, dS(y) \qquad x \in \Omega.$$

The functions F and G are the "Green's functions" of (1). These are known analytically only in the simplest of geometries (when Ω is a circle, a sphere, a half-plane, etc), so a direct solver must build approximations to them given a domain and a differential operator. We observe that the mathematical solution operator is a global operator, so its discrete representation would naturally involve dense matrices. However, these matrices have internal structure that often allows us to represent them and apply them in a computationally efficient manner; analogously to how the Fast Multipole Method efficiently applies a potential evaluation map.

In the context of solvers for oscillatory problems, direct solvers have two highly attractive features: (1) Using a direct solver eliminates the problem of slow convergence of iterative solvers. (While pre-conditioners exist for certain geometries, all such techniques are more or less problem and geometry specific.) (2) When numerically solving scattering problems, it is common that we need to solve a sequence of equations that involve the same geometry and the same operator, but with different body loads and boundary values. For instance, we may for a given shape seek to determine its *radar cross section,* which encodes the reflection from, say, plane waves hitting the shape from different angles. Direct solvers have an inherent advantage in environments like these since the cost of building the solution operator can be amortized over a large number of solves.

High-order discretizations: Beside direct solvers, we argue in the talk that high-order discretizations are essential for successfully addressing high-frequency wave propagation problems. This point has been made by many investigators, and rests on the fact that PDEs such as (1) can be inherently ill-conditioned. If a change in the input data can result in a change in the solution that is larger by, say, a factor 10^3, then we had better use discretizations that resolve the solution to much more than three digits of accuracy. This intrinsic difficulty is also reflected in the well known observation that when low order discretizations are used, the number of discretization points per wavelength required to meet a certain accuracy increases as the domain grows larger.

Combining high-order discretization with direct solvers: The "Hierarchical Poincaré-Steklov (HPS)" method: Having argued that for solving high-frequency problems we need to use both direct solvers and high-order discretizations, we next face the problem that these two methodologies typically do not blend well. For instance, if a standard direct solver for sparse systems such as the nested dissection or multifrontal methods [5, 3, 4] is used to solve the linear systems arising from a finite-difference discretization of (1), then the performance plummets as the discretization order is increased, see, e.g., [6, Table 3].

The second half of the talk was dedicated to presenting a novel discretization scheme that was designed specifically for allowing highly efficient direct solvers to be employed even for methods with high local discretization order. This new scheme is based on a multidomain spectral discretization. For instance, for equation (1) defined on the square $\Omega = [0, 1]^2$, we might use a grid like the one shown in Figure 1. In this figure, the domain is split into 4×4 "leaves" and then on each leaf we place a 7×7 tensor product grid of Chebyshev nodes. The PDE (1) is enforced via collocation on any grid nodes that is interior to a leaf. For each node on a boundary between leaves, we enforce continuity of the normal derivatives. In the talk, we demonstrated that the linear system resulting upon this discretization is remarkably amenable to nested dissection type solvers.

Several numerical examples illustrating the performance of the method were presented. For instance, Table 1 shows the results we recorded when solving (1) on the square $\Omega = [0, 1]^2$ using a local discretization consisting of 21×21 Chebyshev

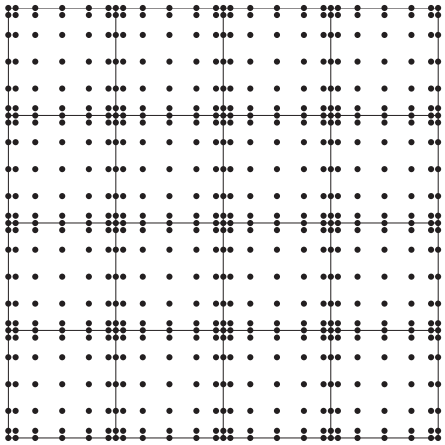

FIGURE 1. Example of a mesh used in the "Hierarchical Poincaré-Steklov (HPS)" method for solving (1) on the domain $\Omega = [0,1]^2$.

N	N_{wave}	t_{build} (sec)	t_{solve} (sec)	E_{pot}	E_{grad}	M (MB)	M/N (reals/DOF)
6561	6.7	0.23	0.0011	2.56528e-10	1.01490e-08	4.4	87.1
25921	13.3	0.92	0.0044	5.24706e-10	4.44184e-08	18.8	95.2
103041	26.7	4.68	0.0173	9.49460e-10	1.56699e-07	80.8	102.7
410881	53.3	22.29	0.0727	1.21769e-09	3.99051e-07	344.9	110.0
1640961	106.7	99.20	0.2965	1.90502e-09	1.24859e-06	1467.2	117.2
6558721	213.3	551.32	20.9551	2.84554e-09	3.74616e-06	6218.7	124.3

TABLE 1. Results from solving (1) on $\Omega = [0,1]^2$ using HPS.

grids (executed on a basic office laptop). In this experiment, the number of points-per-wavelength was kept fixed at 12. t_{build} and t_{solve} refer to the times for the "build stage" (where the approximate solution operator is build) and the "solve stage" (where a solution is computed given Dirichlet data), respectively. E_{pot} is the relative error in the ℓ^∞ norm, and M is the memory required to store the solution operator. We see that there is almost no observable "pollution effect." See [12] for details, with [11] being the original preprint.

The scheme presented has the same asymptotic complexity as classical nested dissection, meaning in two dimensions $O(N^{1.5})$ for the "build stage" and $O(N \log N)$ for the "solve stage." (In 3D, the corresponding numbers are $O(N^2)$ and $O(N^{4/3})$.) For the case where the wave-number is kept fixed as N is increasing, the complexity can be reduced to $O(N)$ for all stages, as shown in [6]. A modification of the scheme that results in better stability for wave-problems, and allows so called "FEM-BEM" coupling is presented in [7]. Preliminary results on the extension to 3D are presented in [10].

Future challenges: While the "HPS" scheme described in the talk provides a path for combining direct solvers with high order discretizations, much work remains to be done. Most importantly, in the situation where the "number of

discretization points per wave-length" is kept fixed as N increases, the current version of HPS does *not* scale linearly, which limits the size of problems that can be handled. (In practice, we estimate that domains up to a couple of hundred of wavelengths in 3D can be handled using current computing machinery.) Direct solvers based on so called "butterfly representations," as described by Eric Michielssen (and discussed in Michael O'Neil's talk) could potentially overcome this problem, and allow for even larger problems to be solved.

The theme of combining high order discretizations with direct solvers is also of high relevance in the context of *boundary integral equation (BIE)* formulations of wave propagation problems. For BIEs in two dimensions, this was explored in [13] and later refined in [8]. The extension to 3D problems is discussed in [9, 1], with techniques for obtaining $O(N)$ complexity in [2] (for the case where the wave-number is kept fixed as N is increased).

References

[1] J. Bremer, A. Gillman, and P.G. Martinsson, *A high-order accurate accelerated direct solver for acoustic scattering from surfaces*, BIT Numerical Mathematics (2014), 1–31 (English).

[2] E. Corona, P.G. Martinsson, and D. Zorin, *An direct solver for integral equations on the plane*, Applied and Computational Harmonic Analysis **38** (2015), no. 2, 284–317.

[3] T.A. Davis, *Direct methods for sparse linear systems*, vol. 2, Siam, 2006.

[4] I.S. Duff, A.M. Erisman, and J.K. Reid, *Direct methods for sparse matrices*, Oxford, 1989.

[5] A. George, *Nested dissection of a regular finite element mesh*, SIAM J. on Numerical Analysis **10** (1973), 345–363.

[6] A. Gillman and P.G. Martinsson, *A direct solver with $o(n)$ complexity for variable coefficient elliptic pdes discretized via a high-order composite spectral collocation method*, SIAM Journal on Scientific Computing **36** (2014), no. 4, A2023–A2046, arXiv.org report #1307.2665.

[7] A. Gillman, A.H. Barnett, and P.G. Martinsson, *A spectrally accurate direct solution technique for frequency-domain scattering problems with variable media*, BIT Numerical Mathematics **55** (2015), no. 1, 141–170 (English).

[8] A. Gillman, P. Young, and P.G. Martinsson, *A direct solver $o(n)$ complexity for integral equations on one-dimensional domains*, Frontiers of Mathematics in China **7** (2012), 217–247, 10.1007/s11464-012-0188-3.

[9] L. Greengard, D. Gueyffier, P.G. Martinsson, and V. Rokhlin, *Fast direct solvers for integral equations in complex three-dimensional domains*, Acta Numer. **18** (2009), 243–275.

[10] S. Hao and P.G. Martinsson, *A direct solver for elliptic PDEs in three dimensions based on hierarchical merging of poincaré-steklov operators*, Journal of Computational and Applied Mathematics **308** (2016), 419 – 434.

[11] P.G. Martinsson, *A composite spectral scheme for variable coefficient helmholtz problems*, arXiv preprint arXiv:1206.4136 (2012).

[12] P.G. Martinsson, *A direct solver for variable coefficient elliptic pdes discretized via a composite spectral collocation method*, Journal of Computational Physics **242** (2013), no. 0, 460 – 479.

[13] P.G. Martinsson and V. Rokhlin, *A fast direct solver for boundary integral equations in two dimensions*, J. Comp. Phys. **205** (2005), no. 1, 1–23.

$\mathcal{DH}^2$-matrix compression of Helmholtz problems

Steffen Börm
(joint work with Christina Börst)

We consider the boundary integral formulation

$$u(x) = \int_{\partial\Omega} g(x,y)\frac{\partial u}{\partial n}(y)\,dy - \int_{\partial\Omega} \frac{\partial g}{\partial n_y}(x,y)u(y)\,dy \qquad \text{for all } x \in \Omega$$

of the Helmholtz equation in a domain Ω. Here

$$g(x,y) = \frac{\exp(\iota\kappa\|x-y\|)}{4\pi\|x-y\|}$$

denotes the fundamental solution. In order to obtain a fast summation scheme, we have to approximate g by a sum of tensor products. If the wave number κ is large, standard approximation schemes like Chebyshev interpolation converge slowly, and this leads to relatively high storage requirements and long computation times.

Following ideas by Brandt [2], Engquist/Ying [3] and Messner/Schanz/Darve [4], we can employ *directional interpolation* to significantly reduce the complexity: we split g into a *plane* wave and a remainder, i.e.,

$$g(x,y) = \exp(\iota\kappa\langle x-y,c\rangle)\underbrace{\frac{\exp(\iota\kappa(\|x-y\|-\langle x-y,c\rangle))}{4\pi\|x-y\|}}_{=:g_c(x,y)}$$

with a direction $c \in \mathbb{R}^3$. It is possible to prove that the modified kernel function g_c is smooth in a cone around the axis c, and we can apply standard interpolation to approximate it in the form

$$g_c(x,y) \approx \tilde{g}_{c,\tau\sigma}(x,y) := \sum_{\nu,\mu=1}^{k} \mathcal{L}_{\tau,\nu}(x)g_c(\xi_{\tau,\nu},\xi_{\sigma,\mu})\mathcal{L}_{\sigma,\mu}(y) \qquad \text{for all } x \in \tau,\ y \in \sigma,$$

where $\tau \times \sigma$ is the domain of interpolation, $(\xi_{\tau,\nu})_{\nu=1}^k$ and $(\xi_{\sigma,\mu})_{\mu=1}^k$ are the interpolation points, and $(\mathcal{L}_{\tau,\nu})_{\nu=1}^k$ and $(\mathcal{L}_{\sigma,\mu})_{\mu=1}^k$ are the corresponding Lagrange polynomials.

Due to

$$\begin{aligned} g(x,y) &= \exp(\iota\kappa\langle x-y,c\rangle)g_c(x,y) \approx \exp(\iota\kappa\langle x-y,c\rangle)\tilde{g}_{c,\tau\sigma}(x,y) \\ &= \sum_{\nu,\mu=1}^{k} \underbrace{\exp(\iota\kappa\langle x,c\rangle)\mathcal{L}_{\tau,\nu}(x)}_{=:\mathcal{L}_{\tau c,\nu}(x)} g_c(\xi_{\tau,\nu},\xi_{\sigma,\mu}) \underbrace{\exp(\iota\kappa\langle -y,c\rangle)\mathcal{L}_{\sigma,\mu}(y)}_{=:\overline{\mathcal{L}_{\sigma c,\mu}(y)}}, \end{aligned}$$

we have found an approximation of g by tensor products. This approach is called *directional interpolation*.

In order to obtain a fast summation scheme, we have to be able to represent the Lagrange polynomials in a nested hierarchy. This goal can be achieved by an

additional approximation step: for $\tau' \subseteq \tau$ and $c' \approx c$, we can apply interpolation again to find

$$\begin{aligned}\mathcal{L}_{\tau c,\nu}(x) &= \exp(\iota\kappa\langle x, c\rangle)\mathcal{L}_{\tau,\nu}(x) = \exp(\iota\kappa\langle x, c'\rangle)\exp(\iota\kappa\langle x, c-c'\rangle)\mathcal{L}_{\tau,\nu}(x)\\ &\approx \exp(\iota\kappa\langle x, c'\rangle)\sum_{\nu'=1}^{k}\underbrace{\exp(\iota\kappa\langle \xi_{\tau',\nu'}, c-c'\rangle)\mathcal{L}_{\tau,\nu}(\xi_{\tau',\nu'})}_{=:e_{\tau' c,\nu'\nu}}\mathcal{L}_{\tau',\nu'}(x)\\ &= \sum_{\nu'=1}^{k} e_{\tau' c,\nu'\nu}\mathcal{L}_{\tau' c',\nu'}(x) \qquad \text{for all } x \in \tau'.\end{aligned}$$

Combining the approximation of g and the approximation of $\mathcal{L}_{\tau c,\nu}$ yields a fast summation method that is similar to the well-known fast multipole scheme, but uses multiple directions c for each subdomain τ.

If we discretize the approximated kernel function, we obtain a $\mathcal{DH}^2$-matrix: the underlying index set $\mathcal{I}$ is split into a cluster tree $\mathcal{T}_\mathcal{I}$, and each cluster $t \in \mathcal{T}_\mathcal{I}$ is associated with a set $\mathcal{D}_t$ of directions. A matrix $G \in \mathbb{C}^{\mathcal{I}\times\mathcal{I}}$ is split into submatrices $G|_{t\times s}$ that are either small or can be expressed in the factorized low-rank form

$$G|_{t\times s} = V_{tc} S_{ts} W_{sc}^*$$

with a direction $c \in \mathcal{D}_t \cap \mathcal{D}_s$ depending on the block $t \times s$ and a *coupling matrix* $S_{ts} \in \mathbb{C}^{k\times k}$.

The cluster bases $(V_{tc})_{t\in\mathcal{T}_\mathcal{I}, c\in\mathcal{D}_t}$ and $(W_{sc})_{s\in\mathcal{T}_\mathcal{I}, c\in\mathcal{D}_s}$ are *nested*, i.e., for all $t' \in \operatorname{sons}(t)$, we can find a direction $c' \in \mathcal{D}_{t'}$ approximating c such that

$$V_{tc}|_{t'\times k} = V_{t'c'} E_{t'c}$$

holds with a *transfer matrix* $E_{t'c} \in \mathbb{C}^{k\times k}$.

Directional interpolation immediately gives rise to $\mathcal{DH}^2$-matrix approximations of the Galerkin stiffness matrices resulting from boundary element discretizations, but the ranks of the approximations are unnecessarily high.

Following [1], we collect all parts of the original matrix $G \in \mathbb{C}^{\mathcal{I}\times\mathcal{I}}$ that will be approximated by V_{tc} in a submatrix G_{tc}. If t is a leaf cluster, we can use a singular value decomposition to find a low-rank approximation

$$G_{tc} \approx V_{tc} V_{tc}^* G_{tc} \tag{1}$$

with an isometric matrix V_{tc} of minimal rank.

Assume now that t is not a leaf cluster. We consider only the case of a binary cluster tree, i.e., we have $\operatorname{sons}(t) = \{t_1, t_2\}$ with $t_1 \neq t_2$. Given $c \in \mathcal{D}_t$, we can find $c_1 \in \mathcal{D}_{t_1}$ and $c_2 \in \mathcal{D}_{t_2}$ approximating c. Once $V_{t_1c_1}$ and $V_{t_2c_2}$ have been computed by recursion, we can consider the matrix V_{tc}. Due to the nested structure, we have

$$V_{tc} = \begin{pmatrix} V_{t_1c_1} E_{t_1c} \\ V_{t_2c_2} E_{t_2c} \end{pmatrix},$$

and we only have to find the transfer matrices E_{t_1c} and E_{t_2c}. Introducing

$$\widehat{V}_{tc} := \begin{pmatrix} E_{t_1c} \\ E_{t_2c} \end{pmatrix}, \qquad Q_{tc} := \begin{pmatrix} V_{t_1c_1} & \\ & V_{t_2c_2} \end{pmatrix}, \qquad \widehat{G}_{tc} := Q_{tc}^* G_{tc},$$

the approximation (1) takes the form

$$\widehat{G}_{tc} \approx \widehat{V}_{tc}\widehat{V}_{tc}^*\widehat{G}_{tc}, \tag{2}$$

and we can construct $\widehat{V}_{tc}$ again by a singular value decomposition. The resulting algorithm takes $\mathcal{O}(n^2k)$ operations to find a $\mathcal{DH}^2$-matrix approximation of a given matrix G, where $n := \#\mathcal{I}$ denotes the matrix dimension.

If the original matrix G is already given in $\mathcal{DH}^2$-matrix form, e.g., obtained by directional interpolation, we can take advantage of the fact that G_{tc} and $\widehat{G}_{tc}$ are matrices of low rank. Using a carefully designed recursive algorithm, we can find weight matrices $Z_{tc} \in \mathbb{C}^{k_G \times k_G}$ and isometric matrices P_{tc} satisfying

$$G_{tc} = V_{G,tc} Z_{tc}^* P_{tc}^*,$$

where $V_{G,tc}$ denotes the cluster basis and k_G denotes the rank of the original representation. Since the factor P_{tc} does not influence the singular values or the left singular vectors, we can drop it and only have to compute the singular value decompositions of matrices with only k_G columns. This approach reduces the complexity to $\mathcal{O}(nk_G^2 \log(n))$.

Numerical experiments illustrate that the $\mathcal{DH}^2$-matrix compression significantly reduces the storage requirements both for the single and the double layer potential operator and may even be applicable to the construction of preconditioners based on approximate LR factorizations.

References

[1] S. Börm and W. Hackbusch. *Data-sparse approximation by adaptive $\mathcal{H}^2$-matrices*, Computing, **69** (2002), 1–35.

[2] A. Brandt, *Multilevel computations of integral transforms and particle interactions with oscillatory kernels*, Comp. Phys. Comm., **65** (1991), 24–38.

[3] B. Engquist and L. Ying. *Fast directional multilevel algorithms for oscillatory kernels*, SIAM J. Sci. Comput., **29(4)** (2007), 1710–1737.

[4] M. Messner, M. Schanz, and E. Darve. *Fast directional multilevel summation for oscillatory kernels based on Chebyshev interpolation*, J. Comp. Sci., **231(4)** (2012), 1175–1196.

Stability of iterated re-interpolation in high-frequency applications

Jens M. Melenk

(joint work with S. Börm)

The numerical treatment of integral operators for high-frequency problems has to address a variety of challenges, e.g., the requirement to store the matrix representation of a discretization and realize a matrix-vector multiplication in log-linear complexity. Algorithms with this feature often rely on two approximation steps: First, a block partition is identified such that each block can be approximation by a low-rank matrix. On the side of analysis, this can be effected by approximating the kernel function in terms of a suitable expansion system (e.g., products of plane waves and polynomials). However, since in the high-frequency setting the number

of such blocks may be too large to ensure log-linear complexity, a second approximation step is necessary that exploits a multilevel structure by suitably relating the chosen expansion system on one level to the one on the next level. We focus on the approximation errors incurred by the second approximation process.

Directional $\mathcal{H}^2$-matrices by interpolation: single-level approximation. We exemplify the situation by the 3D Helmholtz kernel function

$$G(x,y) = \exp(\mathbf{i}k\|x-y\|)\|x-y\|^{-1},$$

where $k > 0$ is assumed to be large. First, let us consider a low-rank approximation of G on the tensor product $B_0^X \times B_0^Y$ of two axis-parallel boxes $B_0^X \subset \mathbb{R}^3$, $B_0^Y \subset \mathbb{R}^3$ that satisfy the *parabolic admissibility condition*

$$k \max\{\operatorname{diam} B_0^X, \operatorname{diam} B_0^Y\}^2 \leq \eta_1 \operatorname{dist}(B_0^X, B_0^Y), \tag{1}$$

$$\max\{\operatorname{diam} B_0^X, \operatorname{diam} B_0^Y\} \leq \eta_2 \operatorname{dist}(B_0^X, B_0^Y). \tag{2}$$

Denote by $c_{B_0^X, B_0^Y}$ the unit vector pointing from the center of B_0^Y to the center of B_0^X, and let $c_0 \in \mathbb{R}^3$ with $\|c_0\| = 1$ be such that

$$k\|c_0 - c_{B_0^X, B_0^Y}\| \max\{\operatorname{diam} B_0^X, \operatorname{diam} B_0^Y\} \leq \eta_3. \tag{3}$$

Then, when denoting by $I_m^B : C(B) \to \mathcal{Q}_m$ the tensor-product Chebyshev interpolation operator mapping into the space of polynomials of degree m (in each variable), one can show (cf. [3, 8, 1, 4]) for $(x,y) \in B_0^X \times B_0^Y$

$$\left| G(x,y) - \exp(\mathbf{i}k\langle x-y, c_0\rangle) I_m^{B_0^X \times B_0^Y} \left(\exp(-\mathbf{i}k\langle x-y, c_0\rangle) G(x,y)\right) \right| \leq \frac{Ce^{-bm}}{\operatorname{dist}(B_0^X, B_0^Y)} \tag{4}$$

for some constants C, $b > 0$ that depend solely on η_1, η_2, η_3. Suitable expansion systems for $B_0^X \times B_0^Y$ are therefore systems of functions of the form

$$L_{B_0^X, i, c}(x) := \exp(\mathbf{i}\langle c, x\rangle) L_{B_0^X, i}(x), \quad i = 1, \ldots, (m+1)^3, \qquad c \in \mathcal{D}_{B_0^X},$$

where $\mathcal{D}_{B_0^X}$ is a set of vectors of unit length that contains the vector c_0, and the functions $L_{B_0^X, i}(x)$, $i = 1, \ldots, (m+1)^3$, form the Lagrange basis of $\mathcal{Q}_m$ associated with Chebyshev interpolation on B_0^X. An analogous expansion system can be associated with B_0^Y.

Directional $\mathcal{H}^2$-matrices by interpolation: multi-level approximation. Assume that a sequence of nested boxes B_ℓ, $\ell = 0, \ldots, L$, is given with the property that, for a fixed $q \in (0,1)$,

$$B_{\ell+1} \subset B_\ell, \qquad \operatorname{diam}_d B_{\ell+1} \leq q \operatorname{diam}_d B_\ell, \qquad d \in \{1,2,3\}; \tag{5}$$

here, $\operatorname{diam}_d A$ denotes the diameter of the set A in the direction of the dth coordinate. Assume the existence of a sequence of vectors c_ℓ, $\ell = 0, \ldots, L$, with

$$\|c_\ell\| = 1 \quad \text{and} \quad k\|c_{\ell+1} - c_\ell\| \operatorname{diam} B_\ell \leq \eta_4, \qquad \ell = 0, \ldots, L-1. \tag{6}$$

These boxes B_ℓ and vectors c_ℓ can be used to define interpolation operators

$$\mathfrak{I}_{B_\ell, c_\ell} f := \exp(\mathbf{i}k\langle x, c_\ell\rangle) I_m^{B_\ell} \left(\exp(-\mathbf{i}k\langle x, c_\ell\rangle) f\right)$$

and the iterated interpolation operators

$$\mathfrak{I}^{iter}_{(B_\ell)_{\ell=1}^L,(c_\ell)_{\ell=1}^L} := \mathfrak{I}_{B_L,c_L} \circ \cdots \circ \mathfrak{I}_{B,c_1}.$$

Theorem 1 *Fix $\widehat{q} \in (q,1)$. Then there exists $\widehat{C} > 0$ depending solely on q such that for all $\pi \in \mathcal{Q}_m$*

$$\| \left(\mathrm{I} - \mathfrak{I}^{iter}_{(B_\ell)_{\ell=1}^L,(c_\ell)_{\ell=1}^L} \right) (\exp(\mathbf{i}k\langle x, c_0\rangle \pi) \|_{L^\infty(B_L)} \leq ((1+\widehat{C}\widehat{q}^m)^L - 1) \|\pi\|_{L^\infty(B_0)}.$$

The algorithm designed in [10] can be analyzed using Theorem 1 as shown in [4]. Underlying this analysis is the observation that, for a parabolically admissible pair (B_0^X, B_0^Y) and sequences $(B_\ell^X)_{\ell=0}^L$, $(B_\ell^Y)_{\ell=0}^L$, $(c_\ell)_{\ell=0}^L$, one has to quantify the accuracy of the approximation

$$G|_{B_L^X \times B_L^Y} \approx \widetilde{G}_{B_L^X \times B_L^Y} := (\mathfrak{I}^{iter}_{(B_\ell^X)_{\ell=1}^L,(c_\ell)_{\ell=1}^L} \circ \mathfrak{I}_{B_0^X,c_0}) \otimes (\mathfrak{I}^{iter}_{(B_\ell^Y)_{\ell=1}^L,(-c_\ell)_{\ell=1}^L} \circ \mathfrak{I}_{B_0^Y,-c_0}) G.$$

[4] shows:

Corollary 1 *Assume that the sequences $(B_\ell^X)_{\ell=0}^L$, $(B_\ell^Y)_{\ell=0}^L$ satisfy the contraction property (5) and that the chosen $(c_\ell)_{\ell=0}^L$ satisfy (6) with both B_ℓ^X and B_ℓ^Y taking the place of B_ℓ there. Then, there are C, b, $C' > 0$ s.t. for $m \geq C' \log(L+1)$*

$$\|G - \widetilde{G}_{B_L^X \times B_L^Y}\|_{L^\infty(B_0^X \times B_0^Y)} \leq C e^{-bm} (\mathrm{dist}(B_0^X, B_0^Y))^{-1}.$$

Extensions to Butterfly algorithms. The approximation result of Theorem 2 can be generalized to certain forms of butterfly algorithms thereby sharpening the analyses of [7] and [9]; details are given in [5].

Let $(x,y) \mapsto \Phi(x,y)$ be a function. Assume that the sequence B_ℓ satisfies (5). Let $(y_{-\ell})_{\ell=0}^L$ be a sequence of points. Define the interpolation operators

$$\widetilde{\mathfrak{I}}_\ell^X f := \exp(\mathbf{i}k\Phi(x, y_{-\ell})) I_m^{B_\ell} (\exp(-\mathbf{i}k\Phi(x, y_{-\ell})) f) \tag{7}$$

and the corresponding iterated version

$$\widetilde{\mathfrak{I}}_L^{X,iter} := \widetilde{\mathfrak{I}}_L^X \circ \cdots \circ \widetilde{\mathfrak{I}}_1^X.$$

One can then prove the following approximation result:

Theorem 2 *Let Φ be real-valued for real arguments and analytic in a complex neighborhood of $B_0^X \times B'$, where the (closed) box $B' \subset \mathbb{R}^3$ contains $y_{-\ell}$, $\ell = 0, \ldots, L$. Assume that the sequence $(B_\ell^X)_{\ell=0}^L$ satisfies the contraction condition (5) and, for some $\eta_5 > 0$,*

$$\mathrm{diam}\, B_{\ell+1}^X \|y_{-\ell} - y_{-(\ell+1)}\| \leq \eta_5/k, \qquad \ell = 0, \ldots, L-1.$$

Then there exist $\widehat{q} \in (q,1)$ and $\widehat{C} > 0$ such that

$$\| \left(\mathrm{I} - \widetilde{\mathfrak{I}}_L^{X,iter} \right) (\exp(\mathbf{i}k\Phi(x, y_0))\pi) \|_{L^\infty(B_L)} \leq ((1+\widehat{C}\widehat{q}^m)^L - 1) \|\pi\|_{L^\infty(B_0)} \quad \forall \pi \in \mathcal{Q}_m.$$

To create separable approximations of $\exp(\mathbf{i}k\Phi(x,y))$, we have to introduce the operators $\widetilde{\mathfrak{I}}_\ell^Y$ analogously to $\widetilde{\mathfrak{I}}_\ell^X$ for a given sequence $(x_{-\ell})_{\ell=0}^L$:

$$\mathfrak{I}_\ell^Y f := \exp(\mathbf{i}k\Phi(x_{-\ell},y))I_m^{B_\ell}\left(\exp(-\mathbf{i}k\Phi(x_{-\ell},y))f\right)$$

and its iterated version $\widetilde{\mathfrak{I}}_L^{Y,iter} := \widetilde{\mathfrak{I}}_L^Y \circ \cdots \circ \widetilde{\mathfrak{I}}_1^Y$.

Corollary 2 *Let $(B_\ell^X)_{\ell=-L}^L$, $(B_\ell^Y)_{\ell=-L}^L$ be two sequences of nested boxes that satisfy the contraction property (5). Assume that Φ is real-valued on $B_{-L}^X \times B_{-L}^Y$ and analytic in a complex neighborhood of $B_{-L}^X \times B_{-L}^Y$. Let $x_\ell \in B_\ell^X$ and $y_\ell \in B_\ell^Y$ satisfy,*

$$\operatorname{diam} B_{\ell+1}^X \|y_{-\ell}-y_{-(\ell+1)}\| + \operatorname{diam} B_{\ell+1}^Y \|x_{-\ell}-x_{-(\ell+1)}\| \le \eta_5/k, \qquad \ell = 0,\dots,L-1.$$

Define the approximation E by

$$\exp(\mathbf{i}k\Phi(x,y) \approx E := (\widetilde{\mathfrak{I}}_L^{X,iter} \circ \widetilde{\mathfrak{I}}_0^X) \otimes (\widetilde{\mathfrak{I}}_L^{Y,iter} \circ \widetilde{\mathfrak{I}}_0^Y)(\exp(\mathbf{i}k\Phi(x,y))).$$

Then, there are constants C, b, $C' > 0$ s.t. for $m \ge C' \log(L+1)$

$$\|\exp(\mathbf{i}k\Phi(x,y)) - E\|_{L^\infty(B_0^X \times B_0^Y)} \le Ce^{-bm}.$$

References

[1] M. Bebendorf, C. Kuske, and R. Venn. Wideband nested cross approximation for Helmholtz problems. *Num. Math.*, 130(1):1–34, 2015.

[2] S. Börm. Directional $\mathcal{H}^2$-matrix compression for high-frequency problems. arXiv:1510.07087

[3] A. Brandt. Multilevel computations of integral transforms and particle interactions with oscillatory kernels. *Comp. Phys. Comm.*, 65:24–38, 1991.

[4] S. Börm and J.M. Melenk. Approximation of the high frequency Helmholtz kernel by nested directional interpolation. arXiv:1510.07189.

[5] S. Börm, C. Börst, and J.M. Melenk. An analysis of a butterfly algorithm (in prep.)

[6] Emmanuel Candès, Laurent Demanet, and Lexing Ying. A fast butterfly algorithm for the computation of Fourier integral operators. *Multiscale Model. Simul.*, 7(4):1727–1750, 2009.

[7] L. Demanet, M. Ferrara, N. Maxwell, J. Poulson, and L. Ying. A butterfly algorithm for synthetic aperture radar imaging. *SIAM J. Imaging Sci.*, 5(1):203–243, 2012.

[8] B. Engquist and L. Ying. Fast directional multilevel algorithms for oscillatory kernels. *SIAM J. Sci. Comput.*, 29(4):1710–1737, 2007.

[9] Stefan Kunis and Ines Melzer. A stable and accurate butterfly sparse Fourier transform. *SIAM J. Numer. Anal.*, 50(3):1777–1800, 2012.

[10] M. Messner, M. Schanz, and E. Darve. Fast directional multilevel summation for oscillatory kernels based on Chebyshev interpolation. *J. Comp. Phys.*, 231(4):1175–1196, 2012.

The Hierarchical Poincaré-Steklov scheme: Oscillatory problems

Adrianna Gillman

(joint work with P.G. Martinsson, A. Barnett, C. Borges and L. Greengard)

Consider the problem of computing the scattered wave u^s that results when a given incident wave u^i (which satisfies the free space Helmholtz equation) impinges upon the region with variable wave speed. Mathematically, the scattered field u^s satisfies the variable coefficient Helmholtz equation

$$\Delta u^s(x) + \kappa^2(1-b(x))u^s(x) = \kappa^2 b(x)u^i(x), \qquad x \in \mathbb{R}^2, \tag{1}$$

and the outgoing Sommerfeld radiation condition

$$\frac{\partial u^s}{\partial r} - i\kappa u^s = o(r^{-1/2}), \qquad r := |x| \to \infty, \tag{2}$$

uniformly in angle. The real number κ in (1) and (2) is the free space wavenumber (or frequency), and the so called "scattering potential" $b = b(x)$ has compact support.

Classic numerical partial differential equation techniques face two big challenges when applied to the problem above for large wavenumber κ. First, the accuracy of finite element and finite difference schemes for the Helmholtz equation is limited by so-called "pollution" (dispersion) error, demanding an increasing number of degrees of freedom per wavelength in order to maintain fixed accuracy as wavenumber κ grows. Second, iterative solvers that are typically used to solve the linear system resulting from discretization are slow to converge due to ill-conditioning. There is much ongoing work to resolve these issues. For example, efficient (both in computational cost and memory) direct solvers have been developed to avoid the convergence issues associated with iterative solvers for highly oscillatory problems.

The authors present a new discretization technique for high frequency scattering problems in variable media. This method which does not observe pollution and has an efficient direct solver called the Hierarchical Poincaré-Steklov (HPS) scheme. The technique uses a classical spectral collocation method, as described in e.g. Trefethen [6], on a collection of disjoint *leaf* boxes whose union is the domain. On each leaf box approximate solution operators and Poincaré-Steklov operators such as Dirichlet-to-Neumann operators are constructed. Then boxes are "glued" together in a hierarchical fashion creating approximate solution and Poincaré-Steklov operators for the union of two boxes. Once this precomputation is complete, new boundary conditions and source functions can be processed by applying the solution operators via a collection of small matrix vector multiplies. The resulting method has computational cost that is asymptotically the same as the nested dissection method [3] but has high order accuracy even for problems with highly oscillatory solutions. For example when applied to the Helmholtz problem with a fixed twelve points per wavelength, the HPS method achieves eight digits of accuracy [5].

In [4], the performance of the HPS method for high frequency variable media problems is investigated. Here we report on the performance for two choices scattering potential $b(x)$:
Lens: A vertically-graded lens (Figure 1(a)), at wavenumber $\kappa = 300$.
Random bumps: The sum of 200 wide Gaussian bumps randomly placed in a box,rolled off to zero (see Figure 1(b)) giving a smooth random potential at wavenumber $\kappa = 160$.

Table 2 reports the number of discretization points N, the points per wavelength ppw, the time for building the direct solver t_{pre}, the time for applying the solver t_{solve} and the relative convergence errors E_{lens} and E_{bumps} for the lens and random bump scattering potentials, respectively. The timings illustrate the pre-asymptotic behavior of the building the direct solver and the extremely small

constant associated with the solve. The errors illustrate that even in the high frequency regime the HPS method is able to achieve spectral accuracy and that the accuracy can be predetermined by choosing the correct number of points per wavelength.

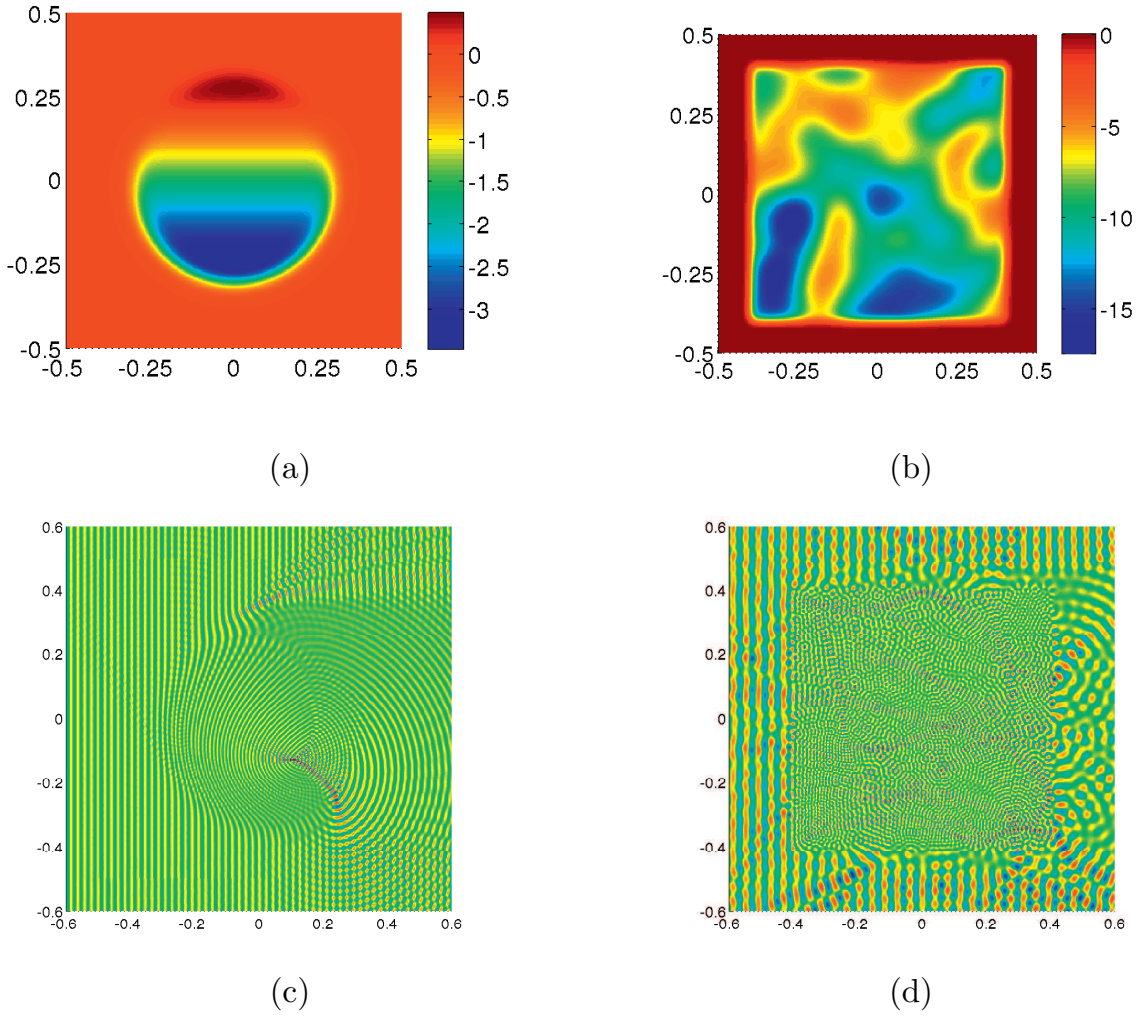

FIGURE 1. Plots of the (a) Lens, and (b) Random bumps scattering potentials as well as the real part of the total field (c), (d) respectively.

With the ability to achieve high accuracy for problems with highly oscillatory solutions and also have an efficient direct solver, the HPS method is ideal for a variety of applications where conditioning and pollution have stagnated progress. Recently it been integrated into a recursive linearization procedure [2] for free space inverse scattering problems[1]. The resulting method was able to recover the media to three digits with over one million PDE solves in two days on a modest server. In the future the method will be applied to a variety of problems including seismic imaging and PDE constrained optimization.

N	ppw	t_{pre}	t_{solve}	E_{lens}	E_{bump}
231361	5	17 s	0.16 s	3e-3	1e-02
923521	10	78 s	0.7 s	2e-7	7e-07
3690241	20	6 m	2.7 s	7e-10	1e-09

TABLE 2. Table reporting the time for computing the direct solver t_{pre}, the time for finding the solution with new boundary data t_{solve}, the relative convergence error E_{lens} and E_{bump} for the lens and bump scattering potentials with *ppw* points per wavelength and N discretization points.

REFERENCES

[1] C. Borges, A. Gillman, and L. Greengard, *Inverse medium scattering in two dimensions with multiple frequency data and multiple angles of incidence*, In review.

[2] Y. CHEN, *Recursive linearization for inverse scattering*, Tech. Report Yale Research Report/DCS/RR-1088, Department of Computer Science, Yale University, New Haven, CT, October 1995.

[3] A. George, *Nested dissection of a regular finite element mesh*, SIAM J. on Numerical Analysis **10** (1973), 345–363.

[4] A. Gillman, A. Barnett, and P. Martinsson, *A spectrally accurate direct solution technique for frequency-domain scattering problems with variable media*, BIT Numerical Mathematics **55** (2014), no. 1, 141–170.

[5] A. Gillman and P.G. Martinsson, *A direct solver with $o(n)$ complexity for variable coefficient elliptic pdes discretized via a high-order composite spectral collocation method*, SIAM J. on Scientific Computing **36** (2014), A2023–A2046.

[6] L.N. Trefethen, *Spectral methods in matlab*, SIAM, Philadelphia, 2000.

Robust periodization of frequency-domain integral equation solvers

ALEX BARNETT

(joint work with Min Hyung Cho, Yuxiang Liu, Adrianna Gillman, Jun Lai, Motoki Kobayashi, Leslie Greengard)

Abstract. Integral equations enable the efficient and accurate numerical solution of wave diffraction from periodic dielectrics or metallic geometries. However, use of the usual quasi-periodic Green's function has certain disadvantages, including its breakdown at certain scattering parameters. I review a spectrally-accurate alternative that combines free-space Green's kernels with a set of auxiliary particular solutions, whose coefficients are solved by imposing periodicity and radiation conditions on a unit cell in the least squares sense. This forms the core of various fast algorithms for the solution of challenging Helmholtz and Maxwell problems in 2D and 3D.

Background and motivation. We seek to solve the scattering of time-harmonic waves at frequency ω from a periodic geometry in 2D or 3D, using boundary integral equation (BIE) methods. The numerous applications include dielectric

diffraction gratings, antennae, meta-materials, photonic crystals, lithography, water waves, and thin-film solar cell design. For simplicity we start with a grating Ω_Λ of disjoint copies of a bounded obstacle $\Omega \subset \mathbb{R}^2$, ie $\Omega_\Lambda := \{\mathbf{x} \in \mathbb{R}^2 : \mathbf{x} + n\mathbf{d} \in \Omega \text{ for some } n \in \mathbb{Z}\}$, where $\mathbf{d} = (d, 0)$ is the lattice vector. An incident plane wave $u^{\mathrm{i}}(\mathbf{x}) = e^{i\mathbf{k}\cdot\mathbf{x}}$ where $\mathbf{k} = (\omega\cos\theta, \omega\sin\theta)$, satisfies the quasi-periodicity condition $u(\mathbf{x}+\mathbf{d}) = \alpha u(\mathbf{x})$ where the Bloch phase is $\alpha = e^{i\omega d\cos\theta}$. The horizontal wavenumbers of plane waves which are quasi-periodic are $\kappa_n = k\cos\theta + 2\pi n/d$. We seek a scattered wave u satisfying the boundary value problem (BVP)

$$(1) \qquad (\Delta + \omega^2)u = 0 \quad \text{in } \mathbb{R}^2\backslash\overline{\Omega_\lambda}$$

$$(2) \qquad u = -u^{\mathrm{i}} \quad \text{on } \partial\Omega_\Lambda$$

$$(3) \qquad u(x,y) = \sum_{n\in\mathbb{Z}} a_n e^{i\kappa_n x + i\sqrt{\omega^2-\kappa_n^2}(y-y_0)}, \quad y \geq y_0, \quad \mathbf{x} = (x,y),$$

$$(4) \qquad u(x,y) = \sum_{n\in\mathbb{Z}} b_n e^{i\kappa_n x + i\sqrt{\omega^2-\kappa_n^2}(y_0-y)}, \quad y \leq -y_0$$

where $y = \pm y_0$ define horizontal lines enclosing $\overline{\Omega}$, and the sign of square-roots are taken positive real or positive imaginary (insuring outgoing or decaying waves respectively). Here (2) insures that the physical wave $u^{\mathrm{i}} + u$ vanishes on $\partial\Omega_\Lambda$, ie, a sound-soft (Dirichlet) boundary condition. (3)–(4) are Rayleigh–Bloch (RB) radiation conditions, the periodic analog of the Sommerfeld condition. A unique solution u to (1)–(4) exists for all ω and $\theta \in (-\pi, 0)$ [3], and is quasi-periodic.

One BIE method to numerically solve the above BVP builds upon the standard BIE method for scattering from a single (non-periodic) obstacle Ω [6]. The latter uses a combined-field indirect BIE representation

$$(5) \qquad u = (\mathcal{D} - i\omega\mathcal{S})\tau$$

where $\mathcal{S}$ and $\mathcal{D}$ are the single- and double-layer potentials based on the free-space kernel $G(\mathbf{x},\mathbf{y}) = \frac{i}{4}H_0^{(1)}(\omega\|\mathbf{x}-\mathbf{y}\|)$, $\mathbf{x},\mathbf{y} \in \mathbb{R}^2$. Then using standard jump relations on $\partial\Omega$ gives the 2nd-kind Fredholm equation $A_0\tau := (\frac{1}{2} + D - i\omega S)\tau = -u^{\mathrm{i}}|_{\partial\Omega}$, which can be solved to give the density τ via the Nyström method with an N-node high-order quadrature. Now, to switch the periodic BVP one may replace G by its quasi-periodic cousin $G_{\mathrm{QP}}(\mathbf{x},\mathbf{y}) = \sum_{m\in\mathbb{Z}} \alpha^m G(\mathbf{x},\mathbf{y}-m\mathbf{d})$, which is a spatial sum over a source lattice. The solution u is then evaluated via (5). This generalizes to doubly-periodic problems in 3D, and is a standard method used by many groups (eg Chandler-Wilde, Arens, Otani–Nishimura [11], Bruno et al [4], etc).

There are three issues with the above approach:

(1) G_{QP} blows up (does not exist) at certain parameter pairs (ω,θ) called Wood anomalies (corresponding to a vanishing vertical wavenumber in the RB expansions), even though the BVP remains well-posed;
(2) pointwise evaluation of $G_{\mathrm{QP}}(\mathbf{x},\mathbf{y})$ introduces an $\mathcal{O}(N^2)$ cost, so is not compatible with fast algorithms;
(3) G_{QP} is difficult to compute accurately. The most popular method involves lattice sums (eg [11]), which can be coupled with a fast algorithm; however,

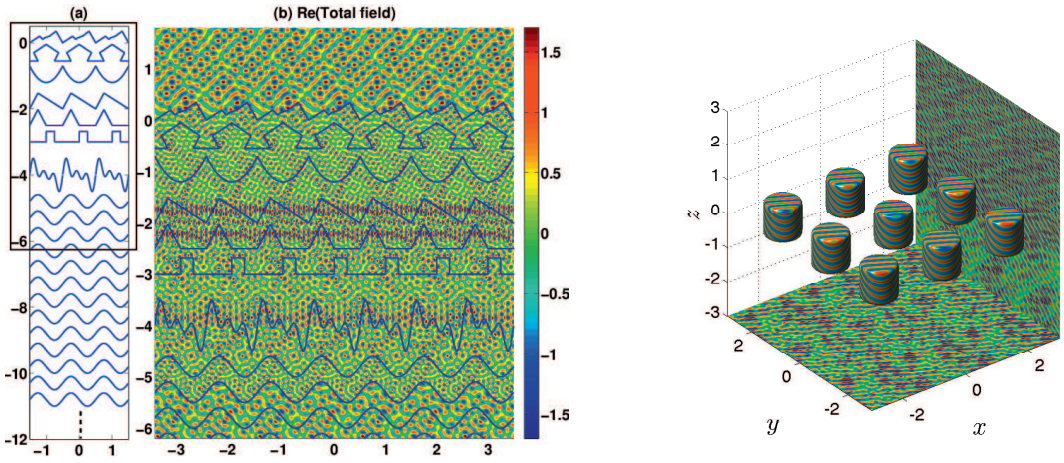

FIGURE 1. Left: scattering from 2D 1000-layer dielectric structure computed by block-tridiagonal direct solver ($N = 6 \times 10^5$ unknowns, 8-digit accuracy, 6 minutes) [5]. Right: 3D electromagnetic scattering from a 13-wavelength doubly-periodic grating of dielectric rounded cylinder shapes ($N = 83000$, 8-digit accuracy, 2 hours) [10].

lattice sums (as do Taylor series) converge in balls, therefore are clumsy if the unit cell has high aspect ratio.

One way around the robustness issue (1) is to use Dirichlet or Neumann half-space versions of $G_{\rm QP}$ which, due to faster decay in the spatial sum, never blow up. However, in multi-layer dielectric problems this would also lead to a non-robust formulation (due to possible resonances of complementary strip-like BVPs), unless *impedance half-space* versions were used, which are difficult to evaluate.

Alternative scheme. We now sketch an alternative which cures all three issues above (for details see [2, 1, 7, 5, 8, 9]). Let $\mathcal{B}$ be a unit cell "box" of width d and vertical extent $[-y_0, y_0]$. We replace (5) by

$$u = \sum_{m\in\{-1,0,1\}} \alpha^m (\mathcal{D}_m - i\omega \mathcal{S}_m)\tau + \sum_{j=1}^{M} c_j \phi_j \ , \tag{6}$$

where $\mathcal{S}_m$ and $\mathcal{D}_m$ indicate layer potentials living on the mth source copy $\partial\Omega + m\mathbf{d}$, while ϕ_j are basis functions (particular solutions) satisfying $(\Delta + \omega^2)\phi_j = 0$ in $\mathcal{B}$. At low frequencies, in 2D, $M \sim 10^2$ and in 3D, $M \sim 10^3$. The unknowns are τ, the vector $\mathbf{c} := \{c_j\}_{j=1}^M$, and the vectors $\mathbf{a}$ and $\mathbf{b}$ containing the coefficients in truncated RB expansions (3)–(4). Three block rows of an *extended linear system* (ELS) are built by i) imposing the boundary condition on the N nodes on $\partial\Omega$, ii) imposing $u_L - \alpha^{-1} u_R = 0$ and $u_{nL} - \alpha^{-1} u_{nR} = 0$, at discrete collocation nodes on L and R, the side walls of $\mathcal{B}$, where n indicates normal derivative, and iii) equating Cauchy data u and u_n at nodes on U and D, the top and bottom walls of $\mathcal{B}$, between (6) and (3) or (4). After stacking $\xi = [\mathbf{c}; \mathbf{a}; \mathbf{b}]$, the ELS takes the

form

$$\begin{bmatrix} A^{\text{near}} & B \\ C & Q \end{bmatrix} \begin{bmatrix} \tau \\ \xi \end{bmatrix} = \begin{bmatrix} -u^{\text{i}}|_{\partial\Omega} \\ \mathbf{0} \end{bmatrix}, \qquad A^{\text{near}} := \tfrac{1}{2} + \sum_{m\in\{-1,0,1\}} (D_m - i\omega S_m),$$

which is rectangular and, due to the last term in (6), ill-conditioned. The block A^{near} is square and well-conditioned. The ELS may be solved in three ways: a) direct dense methods [1]; or by b) eliminating ξ to leave the Schur complement $A_{\text{QP}} = A^{\text{near}} - BQ^{+}C$ (where $Q^{+}C$ is applied in a backward stable fashion), which is an $N \times N$ system for τ that may be solved iteratively using the FMM plus a rank-M correction, as in [8]; or c) eliminating τ (via a fast direct solver to build a compressed A^{-1}) to leave a small dense linear system for ξ. (b) and (c) are "fast."

I now review recent progress based on the above. Method (c) is used in [7], which, since it is rapid for multiple right-hand sides, gives a 600× acceleration over iterative solution via GMRES and FMM. The Schur complements of method (b) are used in each layer of the multilayer dielectric direct solver of [5] (see left panel of Fig. 1). Method (b) with an iterative solver is used for axisymmetric bodies in the 3D acoustic [9] and full Maxwell [10] settings (see right panel).

We sketch a couple of implementation aspects. The choice of ϕ_j may be local expansions (Fourier–Bessel in 2D, or spherical harmonics in 3D) [2, 8, 9, 10], complex plane waves [1, 7], or fundamental solutions (proxy points) [5]. The last two can handle high aspect-ratio unit cells better than lattice sums. Topology turns out to affect the design of a scheme robust at Wood anomalies: for instance, when the obstacles join up to form a continuous layer (as in the left panel), for representations in a half space the non-physical RB condition need not be applied (and in a bounded layer, no RB condition need be applied). This makes method (b) robust, and simplifies the coupled ELS's somewhat [5]. In contrast, for disconnected obstacles, to achieve robustness with method (b) one would have to introduce a fictitious connected interface; we leave this to future work. Methods (a) and (c) are already robust for disconnected obstacles. In the Maxwell case it turns out that one may periodize E_x, E_y and E_z almost as independent scalar fields [10].

Future work. There are many directions in which we expect the above scheme to be useful, including high aspect ratios, various periodicities (eg singly-periodic in 3D), and the design of schemes for the general 3D multilayer dielectric problem. One advantage of our approach is that existing quadrature and FMM libraries built for the non-periodic setting may be exploited as black boxes. Thus a future goal is to release codes for the fast evaluation of potentials due to periodized Helmholtz or Maxwell sources, for all possible dimensions of periodicity in 2D and 3D, which "wrap around" existing free-space FMM libraries. This would decouple the fast periodization task from the choice of quadrature and representation, leaving the last two up to the user. We also leave the interesting problems of non-periodic excitation of periodic geometries, and of local perturbations of periodic geometries, for future research.

References

[1] A. H. Barnett and L. Greengard, *A new integral representation for quasi-periodic scattering problems in two dimensions*, BIT Numer. Math., 51 (2011), pp. 67–90.

[2] A. H. Barnett and L. Greengard, *A new integral representation for quasi-periodic fields and its application to two-dimensional band structure calculations, J. Comput. Phys.*, 229:6898–6914, 2010.

[3] Bonnet-BenDhia, A.-S. and F. Starling. *Guided waves by electromagnetic gratings and non-uniqueness examples for the diffraction problem, Math. Meth. Appl. Sci.*, 17:305–338, 1994.

[4] O. P. Bruno, S. Shipman, C. Turc, and S. Venakides, *Superalgebraically convergent smoothly windowed lattice sums for doubly periodic Green functions in three-dimensional space*, *Proc. R. Soc. Lond. A*, 472, 20160255, 2016.

[5] M. H. Cho and A. H. Barnett, *Robust fast direct integral equation solver for quasi-periodic scattering problems with a large number of layers*, *Opt. Express*, 23(2):1775–1799, 2015.

[6] D. Colton and R. Kress. *Inverse acoustic and electromagnetic scattering theory*, volume 93 of *Applied Mathematical Sciences*, Springer-Verlag, Berlin, second edition, 1998.

[7] A. Gillman and A. Barnett. *A fast direct solver for quasiperiodic scattering problems*, *J. Comput. Phys.*, 248:309–322, 2013.

[8] J. Lai, M. Kobayashi and A. H. Barnett, *A fast and robust solver for the scattering from a layered periodic structure containing multi-particle inclusions*, *J. Comput. Phys.*, 298:194–208, 2015.

[9] Y. Liu and A. H. Barnett, *Efficient numerical solution of acoustic scattering from doubly-periodic arrays of axisymmetric objects*, *J. Comput. Phys.*, 324:226–245, 2016.

[10] Y. Liu, Ph.D thesis, Department of Physics, Dartmouth College, 2016.

[11] Y. Otani and N. Nishimura. *A periodic FMM for Maxwell's equations in 3D and its applications to problems related to photonic crystals, J. Comput. Phys.*, 227:4630–52, 2008.

Butterfly algorithms

Michael O'Neil

Boundary integral equation formulations of the classical PDEs of mathematical physics, namely the Helmholtz and Maxwell's equations, lead to discretized systems which are dense. Denoting the size of these discretized systems by N, their direct solution requires $\mathcal{O}(N^3)$ operations – a cost which is prohibitive for even modest sized problems in three dimensions. However, fast multipole methods for Helmholtz potentials, invented roughly 25 years ago by Greengard and Rokhlin, allow for the rapid application of these systems at a computational cost of $\mathcal{O}(N)$ or $\mathcal{O}(N \log N)$, depending on the driving frequency. This fact, when coupled with iterative linear algebraic solvers, allows for an accelerated solution method to these integral equation formulations, often in the same computational cost when the number of iterations can be controlled.

While asymptotically optimal from a computational point of view, the high-frequency FMM involves several numerical methods involving special functions, filtering, etc. Another, slightly more expensive, alternative to high-frequency FMMs are *butterfly algorithms*, first reported 20 years ago by Michielssen and Boag. This class of algorithms, whose underlying analysis is very similar to FMMs, can be numerically implemented using nothing more that straightforward linear algebraic matrix factorizations. While FMMs rely on the well-separated-ness of groups of sources and targets, butterfly algorithms rely on fixing the *product* of the volume

occupied by those same sources and targets. That is to say, N-body calculations can be accelerated via compressing interactions in a dual-hierarchy where source regions grow larger and target regions shrink by the same factor. These algorithms are very similar to the recent *directional methods*, and contain data movement that is akin to standard implementations of the Fast Fourier Transform.

In this talk I will provide a relatively thorough description of computing the butterfly compression of several oscillatory kernels in one dimension, and give a brief overview of the method in higher dimensions. Then, to highlight some recent research in the area, I will discuss various *butterfly factorizations* and the associated speed-up in precomputation that they admit. Finally, I will work through some of the recent results by E. Michielssen regarding the construction of *fast direct solvers* using butterfly compression. This is very preliminary work, and results are empirical, but it is likely the these algorithms will lead to the first robust fast direct solver for high-frequency wave problems.

Fast solvers for 3D elastodynamic Boundary Element Methods

Stéphanie Chaillat

Scientific Context. The modeling of seismic wave propagation to understand complex phenomena such as site-effects or soil-structure interaction is an active area of research. The difficulties are related to the complexity of the system to model and the large spatial scale of the problems. Currently, 3D simulations are still limited to simplified configurations.

Various numerical methods can be used to simulate seismic wave propagation. The main advantages of the Boundary Element Method (BEM) are to reduce the discretization to the domain boundary and to exactly take into account radiation conditions at the infinite. As a result, BEMs are well suited to deal with problems in (semi-)infinite domains. However standard BEMs lead to a fully-populated influence matrix, and are thus severally limited regarding problems with complex geometries or in a large frequency range. This presentation provides an overview of recent works to improve the efficiency of the method to study elastic wave propagation in large-scale domains.

Fast Multipole Method for problems in a half-space (join work with M. Bonnet). The Fast Multipole Method (FMM) allows one to overcome the drawback of the fully-populated matrix by introducing a fast, reliable and approximate method to compute the linear integral operator [5]. The FMM requires analytic closed-form expression of the fundamental solution to approximate the integral operator and is defined together with the use of an iterative solver. The efficiency of the method has been demonstrated in various fields including in 3D elastodynamics [3]. In a first part, we show the principle of the Fast Multipole Method in 3D elastodynamics and visco-elastodynamics to speed up the solution of the BEM.

A new version of the frequency-domain elastodynamic Fast Multipole-Boundary Element Method (FM-BEM) for semi-infinite media, based on the

half-space Green's tensor (and hence avoiding any discretization of the planar traction-free surface), is then presented. Unlike the full-space Green's tensor, the elastodynamic half-space Green's tensor cannot be expressed using derivatives of the Helmholtz fundamental solution. As a result, multipole expansions of that tensor cannot be obtained directly from known expansions, and are instead derived by means of a partial Fourier transform with respect to the spatial coordinates parallel to the free surface. The obtained formulation critically requires an efficient quadrature for the Fourier integral, whose integrand is both singular and oscillatory. A version custom-tailored for the present needs of a methodology proposed by Bremer et al. [1], which generates generalized Gaussian quadrature rules for specific types of integrals, has been implemented. The accuracy and efficiency of the proposed formulation is demonstrated through numerical experiments. In particular, a complexity significantly lower than that of the non-multipole version is shown to be achieved [2].

Preconditioning the FM-BEM for 3D elastodynamics. The FM-BEM is intrinsically based on an iterative solver. In 3D elastodynamics, it is efficient but the number of iterations can significantly hinder the overall efficiency. In a second part, we present two possible preconditioners: an analytic preconditioner (join work with M. Darbas and F. Le Louër) and a $\mathcal{H}$-LU preconditioner (join work with P. Ciarlet and L. Desiderio).

Analytic preconditioners are in fact a clever integral representation of the scattered field which naturally incorporates a regularizing operator. When considering Dirichlet boundary value problems, the regularizing operator is a high-frequency approximation to the Dirichlet-to-Neumann operator, and is constructed in the framework of the On-Surface Radiation Condition (OSRC) method [4]. The efficiency of such preconditioners is demonstrated for 3D elastodynamic exterior Dirichlet problems.

An alternative approach consists in deriving a low accuracy LU factorization and to use it to precondition the iterative solver. $\mathcal{H}$-matrices [7] permits to approximate the fully-populated BEM matrix by a data-sparse matrix. When used in conjunction with an efficient rank revealing algorithm (for example Adaptive Cross Approximation) it leads to a data-sparse and memory efficient approximation of the original fully-populated BEM matrix. Using the $\mathcal{H}$-matrix arithmetic and low-rank approximations, we derive a fast direct solver. The numerical efficiency and accuracy is assessed on the basis of numerical results obtained for problems having known solutions. We derive then a fast LU solver to precondition the FM-BEM. This type of preconditioner is shown to be moderately efficient in the high frequency regime.

Adaptive mesh strategies (joint work with S. Groth and A. Loseille). Finally, we present the first application of a metric-based anisotropic mesh adaptation strategy within the boundary element method for problems of acoustic wave scattering by three-dimensional obstacles. Traditional mesh adaptation strategies for the BEM rely on Galerkin discretisations of the boundary integral equations. The development and approximation of appropriate error indicators often require the

solution of further, hypersingular, integral equations. These methods utilise the error indicators to mark elements where the error is above a specified tolerance and then refine these elements. The main drawback of such an approach is that the orientation and shape of the elements cannot be modifed. On the other hand, the method we propose is independent of the discretisation technique (e.g., collocation, Galerkin). It completely remeshes the geometry at each refinement step. The shape, size and orientation of elements are modified according to the optimal metric, based on the reconstructed Hessian of the boundary solution. The resulting adaptation is truly anisotropic and we show via a variety of numerical examples that it recovers optimal convergence rates for domains with geometric singularities.

References

[1] J. Bremer, Z. Gimbutas and V. Rokhlin, *A nonlinear optimization procedure for generalized Gaussian quadratures*, SIAM Journal on Scientific Computing **32** (2010), 1761–1788.

[2] S. Chaillat and M. Bonnet, *A new Fast Multipole formulation for the elastodynamic half-space Green's tensor*, Journal of Computational Physics **258** (2014), 787–808.

[3] S. Chaillat, M. Bonnet and J.F. Semblat, *A multi-level fast multipole BEM for 3-D elastodynamics in the frequency domain*, Computer Methods in Applied Mechanics and Engineering **197** (2008), 4233–4249.

[4] S. Chaillat, M. Darbas and F. Le Louër, *Approximate local Dirichlet-to-Neumann map for three-dimensional time-harmonic elastic waves*, Computer Methods in Applied Mechanics and Engineering **297** (2015), 62–83.

[5] R. Coifman, V. Rokhlin, S. Wandzura, *The fast multipole method for the wave equation: A pedestrian prescription*, IEEE Antennas and Propagation Magazine, **35** (1993),7–12.

[6] M. Darbas, E. Darrigrand and Y. Lafranche, *Combining analytic preconditioner and fast multipole method for the 3-D Helmholtz equation*, Journal of Computational Physics **236** (2013), 289–316.

[7] W. Hackbusch, *A sparse matrix arithmetic based on $\mathcal{H}$-matrices. Part I: Introduction to $\mathcal{H}$-matrices*, Computing, **62** (1999), 89–108.

[8] A. Loseille and F. Alauzet, *Continuous mesh framework part I: well-posed continuous interpolation error*, SIAM Journal on Numerical Analysis **49** (2011), 38–60.

Analytic preconditioners for 3D high-frequency elastic scattering problems

Marion Darbas

(joint work with S. Chaillat, F. Le Louër)

Motivations. The aim of this work is to solve numerically 3D high-frequency elastic scattering problems by a bounded rigid obstacle, namely the exterior Navier problem with a Dirichlet boundary condition. To deal with the unbounded characteristic of the computational domain, we choose to apply the integral equation method. It is well-known that the advantage is to reformulate equivalently, through the potential theory, the exterior boundary-value problem as an integral equation on the boundary of the scatterer. The dimension of the problem is thus reduced by one. However, it is well-known also that the discretization by Boundary Element Methods (BEM) of boundary integral equations (BIE) leads to the solution

of large and fully-populated complex linear systems. The solution of these systems can be handled by the GMRES iterative method. To decrease the overall cost of the solver, two complementary ways are investigated: fast methods for the computation of matrix-vector products and preconditioners to speed up the convergence of the solver. The Fast Multipole Method (FMM) permits to overcome the drawback of the fully-populated matrix by introducing a fast and approximate method to compute the linear integral operator. In 3D elastodynamics the FM-BEM has been shown to be efficient [4] with solution times of order $O(N \log N)$ per iteration (where N is the number of BE degrees of freedom). However, the number of iterations in GMRES can significantly hinder the overall efficiency. Preconditioning the FM-BEM is therefore an important practical issue. Preconditioners are prescribed to yield fast convergence independently of both mesh size and frequency.

Methodology. A possible approach consists in constructing analytic preconditioners. The idea is to consider a judicious integral representation of the scattered field which naturally incorporates a regularizing operator. This operator is an approximation of the Dirichlet-to-Neumann (DtN) map. The BIEs arising from this representation are compact perturbations of the identity operator. Such integral formulations can be interpreted as generalizations of the well-known Brakhage-Werner integral equation and Combined Field Integral Equation (CFIE). Several well-conditioned integral equations based on this formalism have already been proposed in acoustics and electromagnetism for ten years (e.g. [1, 2, 3]). In [2], a pseudo inverse of the principal classical symbol of the single layer boundary integral operator - or equivalently the principal classical symbol of the Neumann trace of the double layer boundary integral operator - is used to approach the DtN map in the framework of the On-Surface Radiation Condition methods. This is intuitively natural in view of the Calderón formulas and the compactness of the double layer boundary integral operator.

A preparatory theoretical work has been proposed to adapt such a preconditioning technique to solve Dirichlet exterior scattering problems in 3D-elasticity [6]. The authors suggest strategies to overcome difficulties inherent in elasticity. The double layer boundary integral operator and its adjoint are not compact even for sufficiently smooth boundaries. This implies, according to Calderón formulas, that regularizing the standard BIEs via a pseudo inverse of the single layer boundary integral operator is not sufficient to obtain well-conditioned boundary integral equations. The principal part of the double layer boundary integral operator has also to be taken into account in the preconditioner to regularize the single layer integral operator. It is not an easy task to obtain the expressions of the principal parts of each elementary boundary integral operator. To this end, the tangential Günter derivative plays an important role. The new preconditioned BIEs are well posed at any frequency.

Results. We combine an approximate DtN map as an analytic preconditioner with a FM-BEM solver. The approximations of the DtN map are derived using tools proposed in [6]. They are expressed in terms of surface differential operators, square-root operators and their inverse. Complex Padé rational approximants

provide local and uniform representations of the square-root operators. The additional computational cost of the preconditioner is negligible compared to the cost a FMM accelerated matrix-vector product.

The numerical efficiency of the different proposed preconditioned CFIEs is illustrated for several more or less complex geometries: a unit sphere, an ellipsoid, a cube and a sphere with cavity. An analytical study for the spherical case underlines an "ideal" eigenvalue clustering around the point $(1, 0)$ for the preconditioned CFIEs. This is not the case for the standard CFIE which has small eigenvalues close to zero. The number of GMRES iterations is drastically reduced when the preconditioned CFIEs are considered, independently of the frequency [5].

References

[1] F. Alouges, S. Borel, D.P. Levadoux, *A stable well-conditioned integral equation for electromagnetism scattering*, Journal of Computational and Applied Mathematics, **204**(2) (2007), 440–451.

[2] X.Antoine, M. Darbas, *Generalized combined field integral equations for the iterative solution of the three-dimensional Helmholtz equation*, M2AN, **41** (2007), 147–167.

[3] O.P. Bruno, T. Elling, C. Turc, *Regularized integral equations and fast high-order solvers for sound-hard acoustic scattering problems*, Int. Journal Numerical Methods in Engineering, **91**(10) (2012), 1045–1072.

[4] S. Chaillat, M. Bonnet, J.F. Semblat, *A multi-level fast multipole BEM for 3-D elastodynamics in the frequency domain*, Computer Methods in Applied Mechanics and Engineering, Vol. **197** (2008), 4233–4249.

[5] S. Chaillat, M. Darbas, F. Le Louër, *Fast iterative boundary element methods for high-frequency scattering problems in 3D elastodynamics* , in preparation.

[6] M. Darbas, F. Le Louër, *Analytic preconditioners for the iterative solution of elasticity scattering problems*, M2AS, **38** (2015), 1705–1733.

Software operator frameworks for computational boundary element methods

Timo Betcke

(joint work with Matthew Scroggs, Wojciech Śmigaj)

In recent years there has been tremendous progress for the development of fast boundary integral equation solvers for acoustic and electromagnetic problems. Yet, efficient implementations of these solvers remains a challenging task.

At UCL we are developing the BEM++ library [5] (www.bempp.org), which aims to provide a versatile computational framework for boundary element computations in electrostatics, acoustics and computational electromagnetics. In the following we present a brief overview of the BEM++ operator concept, which allows to model complex boundary integral equationx for challenging high-frequency problems in very simple code snippets.

Operator definitions The basic principle of BEM++ is an operator algebra that knows about domains, ranges and test spaces, and thereby allows complex operations such as operator preconditioning without exposing implementational

issues of the Galerkin discretization to the user. A simple example is the Helmholtz single-layer operator $V : \mathcal{H}^{-1/2}(\Gamma) \to \mathcal{H}^{1/2}(\Gamma)$ given by

$$[V\phi](x) = \int_\Gamma \frac{e^{ik|x-y|}}{4\pi|x-y|}\phi(y)ds(y).$$

To implement the operator we need stable discretizations of the domain space, range space and test space. This is provided by the following BEM++ commands:

```
const_space = bempp.api.function_space(grid, "DUAL", 0)
lin_space = bempp.api.function_space(grid, "B-P", 1)
```

The first space is a space of piecewise constant functions implemented over the dual grid [4]. The second space is the space of standard piecewise linear basis functions over the original grid. The operator can now be defined in BEM++ as

```
slp = bempp.api.operators.boundary.helmholtz.single_layer(
        const_space, lin_space, const_space, k)
```

The first space argument is the domain space of the operator. The second is the range space, and the third is the dual space to the range space, that is the test space. Typically, a Galerkin discretization only needs the domain space and the test space. But the addition of the range space allows us to implement advanced operator concepts. Moreover, this description follows the mathematics in the sense that `const_space` is a suitable discretization of $\mathcal{H}^{-1/2}(\Gamma)$ and `lin_space` discretizes $\mathcal{H}^{1/2}(\Gamma)$ whose dual space is again $\mathcal{H}^{-1/2}(\Gamma)$ for closed boundaries. To demonstrate this concept consider the Helmholtz hypersingular operator mapping from $\mathcal{H}^{1/2}(\Gamma)$ to $\mathcal{H}^{-1/2}(\Gamma)$, and defined in BEM++ as

```
hyp = bempp.api.operators.boundary.helmholtz.hypersingular(
        lin_space, const_space, lin_space, k)
```

A typical form of preconditioning the single-layer operator is multiplying with the hypersingular operator (see e.g. [4]). This can now be easily accomplished with the BEM++ command

```
op = hyp * slp
```

All relevant mappings between the spaces are performed automatically, allowing the user to focus on the Mathematics without needing to deal with details of the underlying Galerkin discretization. These operator concepts have been implemented in BEM++ throughout, including Maxwell problems.

Acoustic High-Frequency Preconditioning As an example we consider a preconditioned Burton Miller formulation for sound-hard scattering of an incoming wave u^{inc} from an obstacle $\Omega \subset \mathbb{R}^3$. The boundary integral formulation is given as

$$\left[\left(\frac{1}{2}I - K\right) - \eta D\right]\phi = u^{inc} - \eta\frac{\partial u}{\partial n}u^{inc}.$$

Here, K is the double layer bounday operator, and D is the hypersingular boundary operator. The parameter η is a coupling constant and is typically chosen as $\eta = \frac{1}{ik}$. The left hand-side operator can easily represented in BEM++ as

```
op = 0.5 * ident - dlp - eta * hyp,
```

where `dlp` is the double layer operator and `hyp` the hypersingular boundary operator defined over spaces of continuous, piecewise linear basis functions. By exchanging η with an operator that approximates the Neumann-To-Dirichlet (NtD) map, a much better conditioned left-hand side can be achieved. BEM++ implements OSRC approximations [1] which can be simply defined as

```
ntd = bempp.api.operators.boundary.helmholtz.osrc_ntd(
          space, k).
```

The resulting preconditioned operator is now given as

```
op = 0.5 * ident - dlp - ntd * hyp.
```

A large-scale example for a problem with over 100 wavelenghts across the domain is presented in [3]. More information on the BEM++ operator algebra can be found in [2].

References

[1] X. Antoine, M. Darbas, *Generalized combined field integral equations for the iterative solution of the three-dimensional Helmholtz equation*, Vol. **41** (2007), 147–167.

[2] T. Betcke, M. Scroggs, W. Śmigaj, *Product algebras for Galerkin discretizations of boundary integral operators and their applications*, in preparation

[3] T. Betcke, E. van 't Wout, P. Gélat, *Computationally efficient boundary element methods for high-frqeuency Helmholtz problems in unbounded domains*, to appear in Modern Solvers for Helmholtz Problems (2016)

[4] R. Hiptmair, *Operator preconditioning*, Computers & Mathematics with Applications, Vol. **52** (2006), 699–706.

[5] W. Śmigaj, T. Betcke, S. Arridge, J. Phillips, M. Schweiger, *Solving boundary integral problems with BEM++*, ACM Transactions on Mathematical Software, Vol. **41** (2015), Article 6.

Hierarchical matrices in scattered data approximation

Sabine Le Borne

Scattered data approximation (SDA) deals with the problem of producing a function, here of type $s : \mathbb{R}^d \to \mathbb{R}$, that in some sense represents some given (typically scattered) data and allows to make predictions at other times/locations/parameter settings. Applications are quite diverse: Surface reconstruction, image compression, numerical solution of PDEs (with their diverse applications), to name just a few.

In the context of this workshop, highly oscillatory problems require (or at least benefit from) high-order discretizations, and kernel-based SDA provides an alternative approach to well-established finite element or finite difference approaches. Furthermore, the resulting discrete operator is (typically) dense and ill-conditioned. Techniques for the efficient representation and preconditioning of (boundary integral) operators for highly oscillatory problems are related and applicable to the discrete operators obtained in SDA.

In a scattered data interpolation problem, the interpolant is typically of the form $s(x) = \sum_{i=1}^{N} c_i b_i(x)$ for some given functions b_i. The coefficient vector $c \in \mathbb{R}^N$ of

the interpolant may be computed as the solution of a linear system $Bc = y$ which results from enforcing the interpolation conditions for the given scattered data. While properties of the matrix B obviously depend on the choice of functions b_i, several of the most commonly used approaches yield highly ill-conditioned, dense matrices B, resulting in a challenge to solve the linear system $Bc = y$, and hence to solve the scattered data interpolation problem. This talk deals with these challenges and some possible strategies for the solution of this system $Bc = y$.

In particular, we study the application of techniques from the $\mathcal{H}$-matrix framework both for the approximation of the system matrix B itself as well as for the construction of preconditioners. $\mathcal{H}$-matrices provide a data-sparse matrix format that permits storage and matrix arithmetic in complexity $\mathcal{O}(N \log^\alpha N)$ for moderate α. It turns out that several typical sets of basis functions from the (scattered data) literature, e.g. Gaussian, (inverse) multiquadrics and thin plate splines, lead to matrices B that fit into this framework, yielding cost-effective approximation schemes of both analytic and algebaric types for the interpolation matrix B as well as its (approximate) LU-factors to be used as a preconditioner in an iterative solver.

References

[1] A. Iske, S. Le Borne, M. Wende, *Hierarchical matrix approximation for kernel-based scattered data interpolation.*, submitted (2016).

On the limitations of sweeping type preconditioners for wave propagation

Martin J. Gander

Sweeping type preconditioners have received a lot of attention over the past few years, following the publication by Engquist and Ying [1]. These preconditioners are however not new: they have their roots in optimal and optimized Schwarz methods and AILU preconditioners, see [2] for an overview and the precise relation between various such techniques, and one has to be careful claiming optimality of such methods for wave propagation problems based on numerical experiments.

To illustrate this, we use here the example that arose during the presentation of Laurent Demanet, namely the one dimensional time dependent wave equation

$$\begin{aligned} &\partial_{tt} u = c^2 \partial_{xx} u \quad \text{in } (0,L)\times(0,T), \\ &\mathcal{B}_l(u) := (\partial_t - c\partial_x)u(0,t) = 0, \quad \mathcal{B}_r(u) := (\partial_t + c\partial_x)u(L,t) = 0, \end{aligned} \tag{1}$$

with appropriate compactly supported initial conditions. For constant wave speed c, the d'Alembert solution is a sum of a left and a right going wave, $u(x,t) = g_l(x+ct) + g_r(x-ct)$, as one can easily see by just introducing it into the wave equation (1). The boundary conditions in (1) are called the transparent (or exact or non-reflecting) boundary conditions, since the outgoing waves satisfy them exactly, $\mathcal{B}_l(g_l) = 0$ and $\mathcal{B}_r(g_r) = 0$, and thus the solution of (1) coincides with the solution of the problem posed on $\mathbb{R}\times(0,T)$.

An optimal Schwarz waveform relaxation method for this problem was defined and analyzed in [3]. It is based on a decomposition of the spatial domain $\Omega := (0, L)$ into non-overlapping subdomains $\Omega_j := (x_{j-1}, x_j)$, $j = 1, 2, \ldots, J$ with $0 =: x_0 < x_1 < \ldots < x_J := L$, and in its alternating (sweeping) version, the method solves at iteration n for a given approximation u_j^{n-1} for $j = 1, 2, \ldots, J$ the forward sweep

$$\begin{aligned} &\partial_{tt} u_j^{n-\frac{1}{2}} = c^2 \partial_{xx} u_j^{n-\frac{1}{2}} \quad \text{in } \Omega_j \times (0, T), \\ &\mathcal{B}_l(u_j^{n-\frac{1}{2}}) = \mathcal{B}_l(u_{j-1}^{n-\frac{1}{2}}), \quad \mathcal{B}_r(u_j^{n-\frac{1}{2}}) = \mathcal{B}_r(u_{j+1}^{n-1}), \end{aligned} \tag{2}$$

where we defined $u_0^{n-\frac{1}{2}} = 0$ and $u_{J+1}^{n-1} = 0$ to simplify the notation. The forward sweep is followed by the backward sweep which solves for $j = J-1, J-2, \ldots 1$

$$\begin{aligned} &\partial_{tt} u_j^{n} = c^2 \partial_{xx} u_j^{n} \quad \text{in } \Omega_j \times (0, T), \\ &\mathcal{B}_l(u_j^{n}) = \mathcal{B}_l(u_{j-1}^{n-\frac{1}{2}}), \quad \mathcal{B}_r(u_j^{n}) = \mathcal{B}_r(u_{j+1}^{n}). \end{aligned} \tag{3}$$

In this alternating version, the algorithm converges in one iteration (a forward sweep followed by a backward sweep) for an arbitrary initial guess u_j^0, as one can see as follows: in the forward sweep, the component of the solution traveling to the right is obtain exactly in each subdomain, since on their left interfaces, no artificial reflections are created. Hence at the end of the forward sweep, $u_J^{\frac{1}{2}} \equiv u$. Now in the backward sweep, this exact solution is just transmitted from right to left, again no reflections are created on the left boundaries of the subdomains, and thus $u_j^1 \equiv u$ also for $j = J-1, J-2, \ldots, 1$. This algorithm is closely related to a block LU decomposition, only the right boundary condition in the block LU factorization corresponds to a Dirichlet condition, see [2]. In a parallel version of the algorithm, convergence is achieved in J iterations, see [3], but then it is essential to use the transparent boundary conditions on both subdomain sides.

Discretizing the wave equation (1) using finite differences, we get

$$\begin{aligned} &\tfrac{u_{i,k+1} - 2u_{i,k} + u_{i,k-1}}{\Delta t^2} = c^2 \tfrac{u_{i+1,k} - 2u_{i,k} + u_{i-1,k}}{\Delta x^2} \qquad 0 \le i \le I, \quad 0 < k < K, \\ &\tfrac{u_{0,k+1} - u_{0,k-1}}{2\Delta t} - c\tfrac{u_{1,k} - u_{-1,k}}{2\Delta x} = 0, \quad \tfrac{u_{I,k+1} - u_{I,k-1}}{2\Delta t} + c\tfrac{u_{I+1,k} - u_{I-1,k}}{2\Delta x} = 0. \end{aligned} \tag{4}$$

If the discretization parameters are chosen precisely at the limit of the CFL condition, $c\frac{\Delta t}{\Delta x} = 1$, this discretization produces the exact solution, as one can verify by introducing the d'Alembert solution consisting of the forward and backward moving waves into (4). This is thus the ideal situation where we can easily check the influence of using transparent transmission conditions or approximations in the discretized algorithm (2,3).

We first show in Figure 1 how one forward and backward sweep generates the exact solution for an example with $J = 6$ subdomains, $L = 6$, $T = 12$, $c = 1$, and $\Delta x = \Delta t = \frac{1}{5}$ so $c\frac{\Delta t}{\Delta x} = 1$, with initial condition $u(x, 0) = 0$ and $\partial_t u(x, 0) = -2(\frac{3}{2} - x)e^{-(\frac{3}{2}-x)^2}$. We see how the algorithm produces the forward moving wave in the forward sweep and then completes the solution in the backward sweep, converging in one iteration as expected for the transparent transmission conditions.

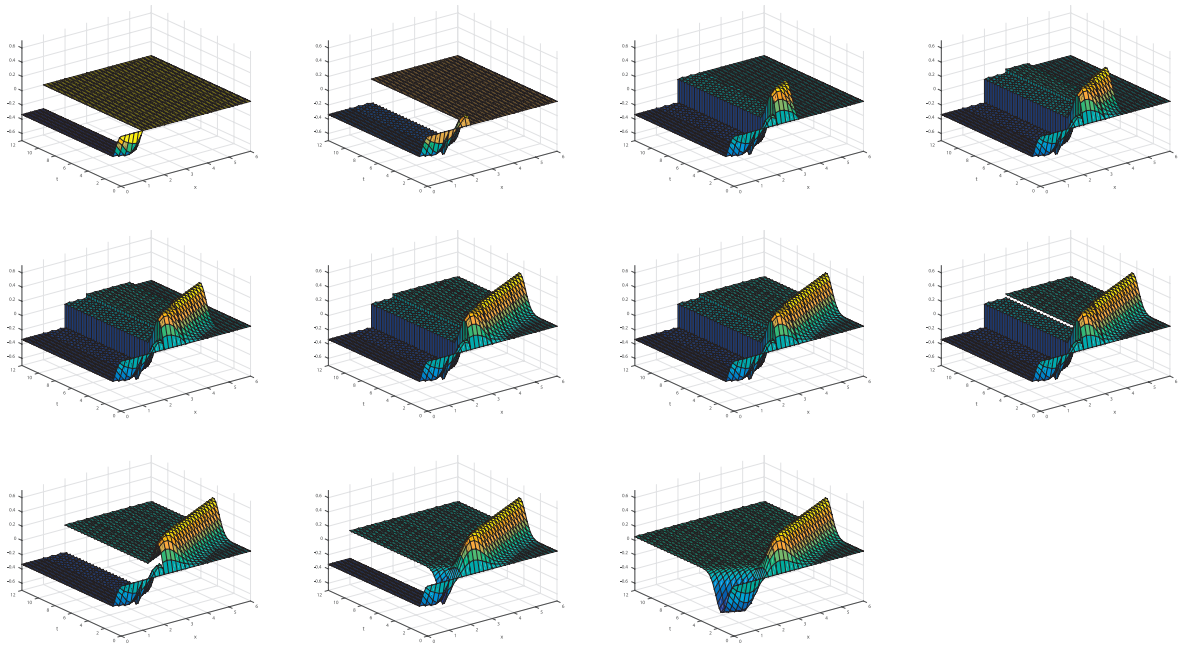

FIGURE 1. The first six panels represent the forward and the last five the backward sweep of one optimal alternating Schwarz waveform relaxation iteration leading to the solution of the problem

The key question we want to address now is what happens if the transparent transmission conditions are approximated. To do so, we apply the algorithm to the error equations, i.e. with zero initial conditions, and we start with a random initial guess on the interfaces. We show in Figure 2 on the left the influence on the convergence behavior of the algorithm when the discretization parameters are chosen either exactly on the CLF, $c\frac{\Delta t}{\Delta x} = \frac{1/10}{1/10} = 1$, or just a little below, $c\frac{\Delta t}{\Delta x} = \frac{3/35}{1/10} = \frac{6}{7}$. We see that when we are exactly on the CFL, the algorithm converges in one double sweep to machine precision, independently of the number of subdomains or the length of the time interval. If we are slightly below however, the first iteration only brings a small error reduction, and then the algorithm seems to stagnate. The spectacular performance is thus intimately related to having the exact (discrete !) transparent boundary condition at the interfaces. In Figure 2 on the right, we show an inhomogeneous numerical example with constant wave speed per subdomain, $c_1 = \frac{1}{2}$, $c_2 = 1$, $c_3 = \frac{2}{5}$, $c_4 = 1$, $c_5 = \frac{3}{10}$ and $c_6 = 1$ (in the case of $J = 12$ subdomains we just repeat the sequence once more), and we use at the interfaces a discretization of the exact transparent boundary condition based on the neighboring subdomain, not taking into account reflections that will come from subdomains with different wave speed further away. When on the CFL for the fastest wave speeds, $c_{\max}\frac{\Delta t}{\Delta x} = \frac{1/10}{1/10} = 1$, the algorithm now converges in a number of iterations that depends on the number (and size) of subdomains

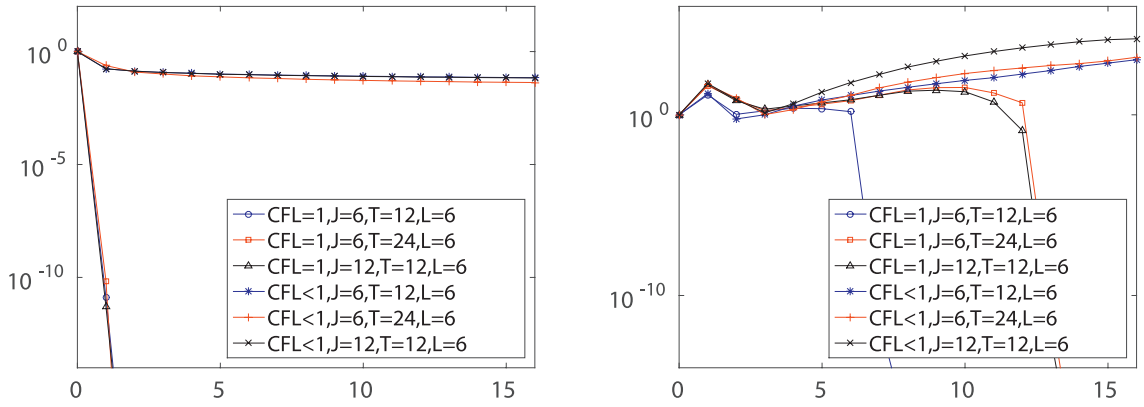

FIGURE 2. Decay of the error as a function of the number of double sweeps when using approximations of the optimal alternating Schwarz waveform relaxation algorithm

and the length of the time interval[1], which can be understood from the number of reflections that have to be taken into account up to the time of interest T, see [3]. The number of reflections would however be infinity in the time harmonic regime, which corresponds to $T = \infty$. If one is slightly below the CFL for all the subdomains, $c_{\max}\frac{\Delta t}{\Delta x} = \frac{3/35}{1/10} = \frac{6}{7}$, the algorithm seems to diverge used as an iterative solver[2]. This could be masked to some extent using Krylov acceleration, but would certainly manifest itself at some point there as well to indicate that this is not an optimal preconditioner any more.

One thus has to be very careful claiming that an optimal solver has been obtained for the time harmonic case just based on numerical experiments, and such preconditioners should always be tested without Krylov acceleration as well, and with random initial guess[3], so convergence problems are not masked initially by a clever polynomial selection of the Krylov method, or just small frequency content.

REFERENCES

[1] B. Engquist, L. Ying *Sweeping preconditioner for the Helmholtz equation: Hierarchical matrix representation*, Comm. Pure Appl. Math. **LXIV** (2011), 697–735.

[2] M.J. Gander, H. Zhang, *Iterative Solvers for the Helmholtz Equation: Factorizations, Sweeping Preconditioners, Source Transfer, Single Layer Potentials, Polarized Traces, and Optimized Schwarz Methods*, submitted to SIAM Review (2016).

[1] It is essential that each subdomain with a CFL less than one has two neighbors with a CFL equal to one for convergence in a finite number of steps.

[2] In this time dependent case, super-linear convergence will set in after a very large number of iteration steps related to the number of time steps, namely after $T/(2\Delta t)$ iterations (e.g. 70 in the first example), due to the waveform relaxation nature of the algorithm, but this would not be the case for a time harmonic formulation that corresponds again to $T = \infty$.

[3] See Subsection 5.2, last paragraph in [4] on how to numerically 'prove' optimality of an algorithm which is in fact not optimal, by just using low frequency content.

[3] M.J. Gander, L. Halpern *Optimal Schwarz Waveform Relaxation for the One Dimensional Wave Equation*, SIAM J. Numer. Anal. **41(5)** (2003), 1643–1681.
[4] M.J. Gander, *Schwarz Methods Over the Course of Time*, ETNA **31** (2008), 228–255.

On domain decomposition preconditioners for finite element approximations of the Helmholtz equation using absorption

Ivan Graham
(joint work with Euan Space, Eero Vainikko)

As a model problem for high-frequency wave scattering, we study the boundary value problem

$$\begin{cases} -(\Delta + k^2)u &= f \quad \text{in } \Omega, \\ \frac{\partial u}{\partial n} - \mathrm{i}ku &= g \quad \text{on } \Gamma, \end{cases} \tag{1}$$

where Ω is a bounded domain in $\mathbb{R}^d$ with boundary Γ. Our results also apply to sound-soft scattering problems in truncated exterior domains. Discretisations of this problem for high wavenumber k are notoriously hard to solve iteratively because the system matrices are complex, non-Hermitian and usually highly non-normal: Information about spectra and condition numbers generally does not give much information about the convergence rates of iterative methods. Here we work with the classcal convergence theory of Eisenstat, Elman and Schultz which requires bounds on the field of values.

There is a strong recent interest on preconditioning (1) using the discrete form of the "shifted Laplace" problem

$$\begin{cases} -(\Delta + k^2 + \mathrm{i}\epsilon)u &= f \quad \text{in } \Omega, \\ \frac{\partial u}{\partial n} - \mathrm{i}\mu(k,\epsilon)u &= g \quad \text{on } \Gamma, \end{cases} \tag{2}$$

for some function μ. Let A, A_ϵ denote the system matrices for discretizations of (1) and (2) respectively, and let B_ε^{-1} denote any (practically useful) approximate inverse for A_ε. It is easy to see that sufficient conditions for B_ε^{-1} to be a good GMRES preconditioner for A are: (i) A_ε^{-1} should be a good preconditioner for A and (ii) B_ε^{-1} should be a good preconditioner for A_ϵ. It is generally observed empirically that (i) holds if the "absorption" parameter $\epsilon > 0$ is not taken too large, while (ii) holds (e.g. for geometric multigrid) provided ϵ is large enough.

In the talk we presented an upper bound on ϵ which ensures that (i) holds, using techniques from PDE analysis of (1) and (2) in the high frequency case [1]. The talk also described lower bounds ε which ensure that (ii) holds, when B_ϵ^{-1} is defined by classical two level additive Schwarz domain decomposition methods on general subdomains with a coarse grid. To obtain the results for (ii) we use a coercivity argument in the natural $k-$dependent Helmholtz energy norm to estimate the field of values of the preconditioned matrix. This analysis is for k arbitrarily large [2].

The gap between the ranges of ϵ which ensure conditions (i) and (ii) hold in practical situations is explored experimentally. The best methods found in practice are either multilevel methods, where relatively fine coarse grids are inverted by inner iterations or one-level methods, where impedance conditions are employed on

subomains. Results were pesented for highly parallelisable variants which combine Dirichlet and impedance local problems on several refinement levels in a hybrid manner, and taking $\varepsilon \sim k$ [3].

In the talk we also presented new work with Eric Chung and Jun Zou (Chinese University of Hong Kong) which provides robustness estimates for domain decomposition methods using impedace local solves for problem (2) with ε close to k. We also presented initial findings of recent work with Stefan Sauter (Zürich) on heterogeneous media problems (where $k = k(x)$).

References

[1] M.J. Gander, I.G. Graham, E.A. Spence, *Applying GMRES to the Helmholtz equation with shifted Laplacian preconditioning: What is the largest shift for which wavenumber-independent convergence is guaranteed?* Numerische Mathematik, 2015. DoI: 10.1007/s00211-015-0700-2

[2] I.G. Graham, E.A. Spence and E. Vainikko, *D*omain decomposition preconditioning for high-frequency Helmholtz problems with absorption. Mathematics of Computation, to appear. `https://arxiv.org/abs/1507.02097`

[3] I.G. Graham, E.A. Spence and E. Vainikko, *Recent Results on Domain Decomposition Preconditioning for the High-frequency Helmholtz Equation using Absorption*, To appear in: Modern Solvers for Helmholtz problems, edited by D. Lahaye, J. Tang and C. Vuik, Springer Geosystems Mathematics series, 2016. `http://arxiv.org/abs/1606.07172`

Aide-mémoire: The method of polarized traces

Laurent Demanet

This note is an overview of the framework in which the method of polarized traces, for computational high-frequency wave propagation, can be understood as the boundary integral version of the optimal Schwarz domain decomposition method of Frédéric Nataf.

1. Polarization

Green's representation formula reads

$$u(x)\chi_\Omega(x) = \int_\Omega G(x,y)f(y)dy + \int_{\partial\Omega} G(x,y)\frac{\partial u}{\partial n}(y)dS_y - \int_{\partial\Omega}\frac{\partial G}{\partial n_y}(x,y)u(y)dS_y. \tag{1}$$

The reasoning above works when $x \in \Omega$, or $x \in \Omega^c$, but does not work when $x \in \partial\Omega$. In that case, a careful analysis of the jump condition for the so-called double layer potential $\int_{\partial\Omega}\frac{\partial G}{\partial n_y}(x,y)u(y)dS_y$ would show that the left-hand side should be $\frac{u(x)}{2}$ when $x \in \partial\Omega$ (provided the latter is smooth enough).

To eliminate exterior unknowns in a scenario when $f = 0$ in Ω^c, the GRF allows to reduce the Sommerfeld radiation condition to

$$0 = -\int_{\partial\Omega} G(x,y)\frac{\partial u}{\partial n}(y)dS_y + \int_{\partial\Omega}\frac{\partial G}{\partial n_y}(x,y)u(y)dS_y, \tag{2}$$

for $x \in \Omega$. It is the exact way of locally encoding the character of a wave that is outgoing at infinity. Its form is independent of the values of $m(x)$ (anywhere away from infinity), or of the boundary condition for $G(x, y)$ in the region $x \in \Omega$ – though of course $G(x, y)$ depends on these choices.

For $x \in \partial\Omega$, we need to mind the extra $\frac{u(x)}{2}$ term again. Then, we can take equation (2) as *the* absorbing boundary condition for $Łu = f$ on Ω, without any approximation. If we denote the single-layer potential by S, and the double-layer potential by D, then we can write equation (2) as $(\frac{I}{2} - D)u = -S\frac{\partial u}{\partial n}$. In what follows, we denote this relation as

$$P_e\left(u, \frac{\partial u}{\partial n}\right) = 0.$$

We call P_e the exterior "polarizer".

2. Localization into subdomains

To discuss domain decomposition, consider the very special scenario where Ω an infinite vertical strip, split in a layered fashion into two strips Ω_1 (left) and Ω_2 (right) meeting at an interface Γ. Respectively call Γ_1 and Γ_2 the left and right infinite edges.

Let $Łu = f$ be posed in Ω without consideration of the boundary condition at infinity[1], and with absorbing boundary condition on $\partial\Omega$, i.e., $P_e\left(u, \frac{\partial u}{\partial n}\right) = 0$ on $\Gamma_1 \cup \Gamma_2$.

Consider two (global) subproblems in Ω,

$$Łv_1 = f\chi_1, \qquad Łv_2 = f\chi_2,$$

with the same homogeneous boundary condition as the original problem, such that $u = v_1 + v_2$. These subproblems can be equivalently formulated in a local fashion, from

- $$Łv_{1,1} = f \qquad \text{in } \Omega_1, \qquad P_2\left(v_{1,1}, \frac{\partial v_{1,1}}{\partial n}\right) = 0 \text{ on } \Gamma,$$
  by simply pushing the right absorbing boundary condition on Γ, and keeping the left boundary condition unchanged. The subscript 2 for P_2 refers to the fact that its Green's function needs to be accurate on Ω_2, though not on Ω_1. Then $v_{1,1} = v_1$ on Ω_1.
- Once the problem for $v_{1,1}$ is solved, let
  $$Łv_{1,2} = 0 \qquad \text{in } \Omega_2, \qquad P_1\left(v_{1,2}, \frac{\partial v_{1,2}}{\partial n}\right) = P_1\left(v_{1,1}, \frac{\partial v_{1,1}}{\partial n}\right) \text{ on } \Gamma,$$
  with an unchanged right boundary condition. Note that, in P_1, there is freedom in changing the problem that gives rise to G_1 in Ω_2, but not in Ω_1. Then $v_{1,2} = v_1$ on Ω_2.

Similarly for v_2, we define the equivalent local subproblems

[1]Or, place those boundary conditions in the definition of the local or global Green's functions

- $$Łv_{2,2} = f \qquad \text{in } \Omega_2, \qquad P_1\left(v_{2,2}, \frac{\partial v_{2,2}}{\partial n}\right) = 0 \text{ on } \Gamma,$$
  with an unchanged right boundary condition. Then $v_{2,2} = v_2$ on Ω_2.
- Once the problem for $v_{2,2}$ is solved, let

$$Łv_{2,1} = 0 \qquad \text{in } \Omega_1, \qquad P_2\left(v_{2,1}, \frac{\partial v_{2,1}}{\partial n}\right) = P_2\left(v_{2,2}, \frac{\partial v_{2,2}}{\partial n}\right) \text{ on } \Gamma,$$

with an unchanged left boundary condition. Then $v_{2,1} = v_2$ on Ω_1.

3. Optimal Schwarz sequence

We may group the computation of the four local subproblems in a more efficient fashion that results in 3 subproblems only.

(1) Solve for $v_{1,1}$ as earlier, and for simplicity call it v_1;
(2) On Ω_2, consider the combined subproblem with both (i) a non-zero right-hand side, and (ii) the condition on Γ that transmits v_1, namely

$$Łu_2 = f \qquad \text{in } \Omega_2, \qquad P_1\left(u_2, \frac{\partial u_2}{\partial n}\right) = P_1\left(v_1, \frac{\partial v_1}{\partial n}\right) \text{ on } \Gamma,$$

with an unchanged right boundary condition. Then $u_2 = v_{1,2} + v_{2,2} = v_1 + v_2$ on Ω_2, as desired.
(3) On Ω_1, solve

$$Łu_1 = f \qquad \text{in } \Omega_1, \qquad P_2\left(u_1, \frac{\partial u_1}{\partial n}\right) = P_2\left(u_2, \frac{\partial u_2}{\partial n}\right) \text{ on } \Gamma,$$

with an unchanged left boundary condition. Note that, in this last step only, there is freedom to require another condition on Γ, such as $u_2 = u_1$.

For general domain decomposition, this sequence is a double sweep that computes v_1 through v_{n-1} (like a forward substitution), then u_n to u_1 (like a backward substitution). The requirements for this sequence to be exact is that the G_j used in P_j should be exact in $\Omega_{j\sim}$, the union of all the subdomains to the right of Ω_j for the forward sweep, and exact in $\Omega_{\sim j}$, the union of all the subdomains to the left of Ω_j for the backward sweep.

4. Integral version of the optimal Schwarz sequence

Denote the traces of u respectively as u_L, u_Γ, u_R, and the traces of $\frac{\partial u}{\partial n}$ as $\lambda_L, \lambda_\Gamma, \lambda_R$. Continue to consider the problem on Ω, with $P_1(u_L, \lambda_L) = P_2(u_R, \lambda_R) = 0$. In its integral form, the optimal Schwarz sequence may be called the method of polarized traces, and becomes

(1)

$$\begin{bmatrix} v_\Gamma \\ \mu_\Gamma \end{bmatrix} = \begin{bmatrix} \int_{\Omega_1} G_1 f \\ \int_{\Omega_1} \frac{\partial G_1}{\partial n} f \end{bmatrix}.$$

These traces are polarized right-going by construction, i.e., $P_2(v_\Gamma, \mu_\Gamma) = 0$.

(2)
$$\begin{bmatrix} u_R \\ \lambda_R \end{bmatrix} = \begin{bmatrix} \int_{\Omega_2} G_2 f \\ \int_{\Omega_2} \frac{\partial G_2}{\partial n} f \end{bmatrix} + \begin{bmatrix} D & -S \\ N & -D^* \end{bmatrix} \begin{bmatrix} v_\Gamma \\ \mu_\Gamma \end{bmatrix},$$
where S, D, D^*, N are the usual layer potentials. These traces are polarized right-going by construction, i.e., $P_2(u_R, \lambda_R) = 0$.

(3)
$$\begin{bmatrix} u_\Gamma \\ \lambda_\Gamma \end{bmatrix} = \begin{bmatrix} v_\Gamma \\ \mu_\Gamma \end{bmatrix} + \begin{bmatrix} \int_{\Omega_2} G_2 f \\ \int_{\Omega_2} \frac{\partial G_2}{\partial n} f \end{bmatrix}.$$
The second term in the right-hand side contains the left-polarized traces.

(4)
$$\begin{bmatrix} u_L \\ \lambda_L \end{bmatrix} = \begin{bmatrix} \int_{\Omega_1} G_1 f \\ \int_{\Omega_1} \frac{\partial G_1}{\partial n} f \end{bmatrix} + \begin{bmatrix} D & -S \\ N & -D^* \end{bmatrix} \begin{bmatrix} u_\Gamma \\ \lambda_\Gamma \end{bmatrix}.$$
These traces are polarized left-going by construction, i.e., $P_1(u_L, \lambda_L) = 0$.

The integral formulation presents a potential advantage: The integral equations no longer need to be understood as a sequence, they can be viewed as a self-contained system of equations at the interfaces/boundaries. The Schwarz sequence is then an exact double-sweep inverse for this system. If the Green's function G_j is modified liberally in Ω_j^c (rather than $\Omega_{j\sim}$ or $\Omega_{\sim j}$ as explained earlier), then the exactness of the double sweep is lost, *but* the integral system for the polarized traces remains exact. We believe that this property of algebraic exactness is desirable in the method of polarized traces.

Reporter: Timo Betcke

Participants

Prof. Dr. Alex H. Barnett
Department of Mathematics
Dartmouth College
6188 Kemeny Hall
Hanover, NH 03755-3551
UNITED STATES

Dr. Timo Betcke
Department of Mathematics
University College London
Gower Street
London WC1E 6BT
UNITED KINGDOM

Prof. Dr. Steffen Börm
Lehrstuhl Scientific Computing
Christian-Albrechts-Universität für Informatik
Christian-Albrecht-Platz 4
24118 Kiel
GERMANY

Dr. Stéphanie Chaillat-Loseille
ENSTA ParisTech
828, Boulevard des Marechaux
91762 Palaiseau Cedex
FRANCE

Dr. Marion Darbas
LAMFA
Université Picardie Jules Verne
33 rue Saint-Leu
80000 Amiens
FRANCE

Prof. Dr. Laurent Demanet
Department of Mathematics
Massachusetts Institute of Technology
77 Massachusetts Avenue
Cambridge, MA 02139-4307
UNITED STATES

Prof. Dr. Martin Gander
Département de Mathématiques
Université de Geneve
Case Postale 64
2-4 rue du Lievre
1211 Genève 4
SWITZERLAND

Prof. Dr. Adrianna Gillman
Department of Mathematics
Rice University
P.O. Box 1892
Houston, TX 77005-1892
UNITED STATES

Prof. Dr. Ivan G. Graham
Dept. of Mathematical Sciences
University of Bath
Claverton Down
Bath BA2 7AY
UNITED KINGDOM

Prof. Dr. Sabine Le Borne
Institut für Mathematik (E-10)
Technische Universität
Hamburg-Harburg
Am Schwarzenberg-Campus 3
21073 Hamburg
GERMANY

Prof. Dr. Per-Gunnar Martinsson
Dept. of Applied Mathematics
University of Colorado at Boulder
Campus Box 526
Boulder, CO 80309-0526
UNITED STATES

Prof. Dr. Jens M. Melenk
Institut f. Analysis & Scientific Computing
Technische Universität Wien
Wiedner Hauptstrasse 8 - 10
1040 Wien
AUSTRIA

Prof. Dr. Michael O'Neil
Courant Institute of Mathematical Sciences
New York University
251, Mercer Street
New York, NY 10012-1110
UNITED STATES

Sunli Tang
Courant Institute of Mathematical Sciences
New York University
251, Mercer Street
New York, NY 10012-1110
UNITED STATES